Exploring the NCS-382 Scaffold for CaMKIIα Modulation: Synthesis, Pharmacology, and Biophysical Characterization of Ph-HTBA as a Novel High-Affinity Brain-Penetrant Stabilizer of the CaMKIIα Hub Domain

Yongsong Tian[†,‡], Mohamed A. Shehata[†,‡], Stine Juul Gauger[†], Carolina Veronesi[†], Louise Hamborg[†], Louise Thiesen[†], Jesper Bruus-Jensen[†], Johanne Schlieper Royssen[†], Ulrike Leurs[†], Anne Sofie G. Larsen[†], Jacob Krall[†], Sara Solbak[†], Petrine Wellendorph[†,], Bente Frølund[†,*]*

[†] Department of Drug Design and Pharmacology, Faculty of Health and Medical Sciences, University of Copenhagen, Universitetsparken 2, DK-2100 Copenhagen, Denmark.

KEYWORDS γ-hydroxybutyric acid (GHB), Ca^{2+}/calmodulin-dependent protein kinase II alpha (CaMKIIα), (*E*)-2-(5-hydroxy-5,7,8,9-tetrahydro-6*H*-benzo[7]annulen-6-ylidene) acetic acid (NCS-382), (*E*)-2-(5-hydroxy-2-phenyl-5,7,8,9-tetrahydro-6*H*-benzo[7]annulen-6-ylidene)acetic acid (Ph-HTBA), structure-based design, radioligand binding, biophysical assay panel, brain permeability

ABSTRACT Ca^{2+}/calmodulin-dependent protein kinase II alpha (CaMKIIα) is a brain-relevant kinase and an emerging drug target for ischemic stroke and neurodegenerative disorders. Despite various reported CaMKIIα inhibitors, their usefulness is limited by low subtype selectivity and brain permeability. (*E*)-2-(5-Hydroxy-5,7,8,9-tetrahydro-6*H*-benzo[7]annulen-6-ylidene)acetic acid (NCS-382) is structurally related to the proposed neuromodulator, γ-hydroxybutyric acid, and is a brain-penetrating high nanomolar-affinity ligand selective for the CaMKIIα hub domain. Herein, guided by *in silico* approaches, we synthesized the first series of

NCS-382 analogs displaying improved affinity and preserved brain permeability. Specifically, we present Ph-HTBA (**1i**) with enhanced mid-nanomolar affinity for the CaMKIIα binding site and a marked hub thermal stabilization effect along with a distinct CaMKIIα Trp403 flip upon binding. Moreover, Ph-HTBA has good cellular permeability and low microsomal clearance and shows brain permeability after systemic administration to mice, signified by a high Kp,uu value (0.85). Altogether, our study highlights Ph-HTBA as a promising candidate for CaMKIIα-associated pharmacological interventions and future clinical development.

Introduction

γ-Hydroxybutyric acid (GHB) is an endogenous substance and a metabolite of γ-aminobutyric acid (GABA), which is present in the central nervous system (CNS) in micromolar concentrations.[1] It is notoriously known as a recreational drug (Fantasy), but is also clinically used in narcolepsy and alcoholism therapy.[2-4] Recently, by means of pharmacological and crystallographic approaches, we reported that Ca^{2+}/calmodulin dependent protein kinase II alpha (CaMKIIα) harbors a specific high-affinity binding site for GHB analogs deep in the hub domain.[5] Importantly, this finding is further substantiated with the selective binding of GHB radioligands to CaMKIIα, and a high-resolution (2.2 Å) crystal structure of a tetradecameric CaMKIIα hub protein bound with a high-affinity ligand, 5-hydroxydiclofenac (5-HDC, Figure 1A) (PDB: 7REC).[5, 6]

CaMKII is an oligomeric protein kinase assembled by 12-14 monomers in a double-layered ring.[7] Structurally, each monomer consists of an *N*-terminal catalytic domain (including the ATP binding site), a self-regulatory domain (containing the Ca^{2+}/CaM binding site and essential phosphorylation sites), and a *C*-terminal association domain (the hub domain) connected *via* a variable linker.[7] In the brain, CaMKII is predominantly composed of

heteromeric complexes consisting of both CaMKIIα and CaMKIIβ.[8-10] CaMKIIα, an abundant kinase in the brain, regulates the synaptic signaling through phosphorylation of ion channels and neurotransmitter receptors, and is a major player in the integration of Ca^{2+} inputs regulated by autophosphorylation.[11] For that reason, it is involved in long-term potentiation (LTP) and synaptic plasticity,[12, 13] and thus modulates brain functions such as learning and memory.[11, 14] This is further validated by the observation that CaMKIIα knock-out mice are learning deficient and display reduced LTP.[12, 15] Due to its central role in regulating synaptic functions, CaMKIIα has been shown to be pathophysiologically involved in ischemia[16, 17] and neurodegenerative disorders, e.g. Alzheimer's[18] and Parkinson's disease[19]. Moreover, the dysregulation of CaMKIIα activity has been reported to be associated with intellectual disability.[20] Together, this makes CaMKIIα an emerging drug target, however, so far, largely under-explored.

Although various CaMKII inhibitors have been developed,[21] the majority of them targets the ATP binding site,[22, 23] the substrate-binding T-site,[24] or the Ca^{2+}/CaM interaction site.[25] These sites are generally highly conserved among CaMKII subtypes, resulting in a very low degree of selectivity for reported CaMKII inhibitors. Accordingly, there is a need for CaMKII subtype-selective ligands for specific modulation and therapy. The central hub domain of CaMKIIα has been reported as an allosteric regulator for kinase activity,[26] and to be subject to activation-triggered destabilization and subunit exchange, potentially also regulating function.[27, 28] Notably, a six-mutant (6x) human hub domain that is highly stabilized in this regard has been engineered and used to aid structural investigations.[5, 29] Through crystallographic and biophysical methods, we recently presented a possible mechanism by which the binding of ligands to the hub cavity produces a pronounced thermal stabilization of the hub oligomer complex. Additionally, for 5-HDC, a structural movement of the CaMKIIα-specific residue Trp403 at the upper edge of the pocket, causing a significant conformational change of the holoenzyme, has been detected.[5] Trp403 is situated right next to the alpha helix (αD, 394–402,

CaMKIIα human numbering) which is implicated in the stabilization of the lateral interaction between hub subunits, which also contains several aromatic amino acids.[30] In particular, such hub stabilizing effect is stipulated to help confer sustained neuroprotection in the brain.[5] This highlights the hub domain as a novel mechanistic way into specific pharmacological modulation of the CaMKII activity.

Among several reported structural classes of GHB analogs exhibiting mid-to-high nanomolar affinity for the CaMKIIα hub domain,[5, 6, 31-34] 3-hydroxycyclopenten-1-enecarboxylic acid (HOCPCA, Figure 1A) and (*E*)-2-(5-hydroxy-5,7,8,9-tetrahydro-6*H*-benzo[7]annulen-6-ylidene) acetic acid (NCS-382, Figure 1A) are brain permeable and represent favorable ligands for *in vivo* studies.[35-37] NCS-382 was first developed as a selective semi-rigid GHB analog toward, at that time, the unidentified high-affinity GHB binding sites.[38] It displays a ten-fold higher affinity (K_i 0.34 μM) than GHB (K_i 4.3 μM) in [^{3}H]NCS-382 competition binding assays to CaMKIIα in rat cortical homogenates,[39] and proves to permeate the blood-brain barrier (BBB) as a substrate of the monocarboxylate transporter 1 (MCT1) along with yet other unidentified pathways (e.g., passive diffusion).[37] Despite comprehensive pharmacological studies, the potential of NCS-382 for further ligand development to achieve enhanced binding affinity and pharmacokinetic properties was unexplored, limited by the lack of a crystal structure to guide the work.

Herein, we present the design, synthesis, and pharmacological evaluation of a novel series of NCS-382 analogs (**1a**–**n**). A detailed *in silico* rational design and molecular mode-of-action analysis as well as a structure-affinity relationship (SAR) study of the developed ligands are presented. Specifically, we highlight the 2-phenyl analog, Ph-HTBA (**1i**), as a selective, brain-penetrating modulator for CaMKIIα with approximately four times improved affinity compared to NCS-382. By applying an in-house established biophysical assay panel for the CaMKIIα hub domain (using both wild-type and 6x mutant purified protein), we further confirm that Ph-

HTBA binds directly to and improves the thermal stability of the CaMKIIα hub domain, and also involves the movement of Trp403 in the upper hub cavity upon binding. Together, Ph-HTBA represents an important and promising ligand in further pharmacological intervention of CaMKIIα, and is also a potential molecule for future clinical development.

Results and Discussion

Ligand Design. The core chemical scaffold of NCS-382 comprises a 6,7,8,9-tetrahydro-5*H*-benzo[7]annulene ring system. To probe the binding pocket around the scaffold, chemical groups at the three designated positions in the phenyl ring: C-1, C-2 and C-3 (Figure 1B) were explored. In line with previous findings,[33, 34] computational docking studies pointed out a hydrophobic sub-pocket in the upper part of the GHB binding cavity, where large and aromatic substituents were tolerated. Therefore, C-1 and C-2 positions, which point toward that part of the binding pocket were generally probed with larger substituents and extensions reaching further up. For the C-3 position, only one small and one large substituent were probed, since this area of the pocket has never been previously explored by any other scaffolds. For the aliphatic ring system, docking studies show a tight fit in the pocket, and no further substituents were synthetically plausible. The upper part of the aliphatic ring (purple arrows, Figure 1B) was deemed equivalent to C-1 in the aromatic ring as attachment points for introducing extensions reaching the upper hydrophobic sub-pocket. However, since the aliphatic ring of NCS-382 generally presents much more challenging chemistry, no analogs probing this ring were suggested for further design.

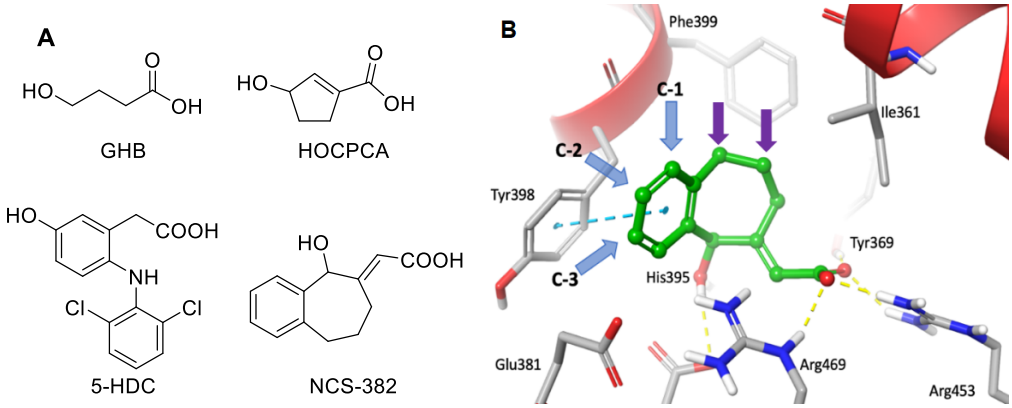

Figure 1. (A) Chemical structures of γ-hydroxybutyric acid (GHB), 3-hydroxycyclopenten-1-enecarboxylic acid (HOCPCA), 5-hydroxydiclofenac (5-HDC) and (*E*)-2-(5-hydroxy-5,7,8,9-tetrahydro-6*H*-benzo[7]annulen-6-ylidene)acetic acid (NCS-382). (B) Docked binding pose of NCS-382 (green) in the pocket of CaMKIIα (backbone – red, amino acids – grey). Designated labels C-1, C-2 & C-3 with blue arrows represent positions for the suggested new design of NCS-382 analogs, whereas the positions labeled with purple arrows in the aliphatic ring were deemed equivalent to C-1 in the aromatic ring as attachment points yet unexplored. Aromatic interactions are depicted in cyan dashed lines and hydrogen bonds in dashed yellow lines.

Although stereochemistry plays an important role in the molecular recognition and affinity of the NCS-382 scaffold, the racemic NCS-382 mixture merely displayed a two-fold lower affinity than that of the (*R*)-stereoisomer, but a six-fold higher affinity versus its (*S*)-stereoisomer.[40] Combined with laborious isolation of stereoisomers, we decided to retain the developed ligands as racemates. In total, fourteen novel NCS-382 analogs (**1a**–**n**) were successfully synthesized and pharmacologically characterized for their binding affinities.

Synthesis of Target Compounds. New NCS-382 analogs **1a**–**n** were synthesized as depicted in Scheme 1. Inspired by Murineddu et al.,[41] benzocycloheptanones **5a**–**e** were prepared from corresponding benzaldehydes **2a**–**e** through a three-step synthetic route using optimized

conditions. Wittig condensation of **2a**–**e** using phosphonium bromide gave phenylpentenoic acids **3a**–**e**. A two-step sequence involving hydrogenation of **3a**–**e** followed by an intramolecular cyclization generated benzocycloheptanones **5a**–**e**. By using brominated intermediates **5a**–**c**, diversification of functional groups on the phenyl ring of the core structure was initiated. For example, palladium-catalyzed stannylation of **5b** provided the analogous tributylphenylstannane, which was subsequently converted to the fluorinated (**5f**) or iodinated derivative (**5g**) through silver-catalyzed fluorination[42] or direct iodination[43, 44], respectively. In addition, starting from **5a**–**c**, a series of aryl substituents was introduced to the designated C-1, C-2, and C-3 positions of the NCS-382 scaffold *via* cross-coupling reactions. Intermediates **5a**–**c** were coupled with phenylboronic acid *via* Suzuki–Miyaura reaction, affording phenyl substituted compounds **5h**–**j**. Similarly, *trans*-styryl compounds **5k**–**m** were obtained from **5a**–**b** *via* Heck reaction. Subsequently, **5k** was subjected to a palladium-catalyzed hydrogenation to afford **5n**. Noteworthy, with the intention to prepare the final 2-phenyl NCS-382 analog **1i** (Ph-HTBA) in gram-scale for further *in vitro* and *in vivo* studies, **5i** was also alternatively synthesized from **2i** by employing the three-step synthetic route as above-illustrated (Scheme 1). This strategy was relatively more cost-effective by avoiding the use of expensive palladium catalyst during Suzuki–Miyaura reaction. Next, Claisen–Schmidt condensation of benzocycloheptanones **5a**–**n** with glyoxylic acid furnished **6a**–**n**, whereof α,β-unsaturated ketones were chemo-selectively reduced to allyl alcohols according to Luche reduction, giving target NCS-382 analogs **1a**–**n**.

Scheme 1. Synthesis of NCS-382 Analogs 1a–n[a]

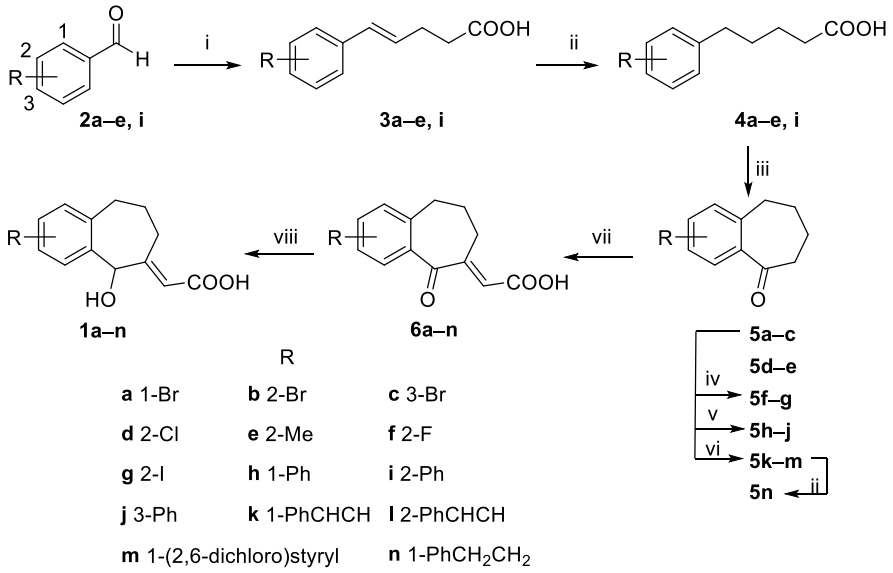

[a]Reagents and conditions: i) (3-carboxypropyl)triphenylphosphonium bromide, NaHMDS, -78 °C to rt; ii) Pd/C, H_2, EtOAc; iii) (a) polyphosphoric acid, 100 °C or 130 °C and (b) 2N NaOH; iv) (a) Pd $(PPh_3)_4$, bis(tributyltin), toluene, reflux and (b) for **5f**: Ag_2O, $NaHCO_3$, Selectfluor, acetone, reflux, or for **5g**: I_2, THF, 0 °C; v) phenylboronic acid, $Pd(PPh_3)_4$, K_2CO_3, DMF, H_2O, reflux; vi) styrene or 2,6-dichlorostyrene, $Pd(OAc)_2$, PPh_3, K_2CO_3, DMF, 110 °C; vii) glyoxylic acid monohydrate, NaOH, EtOH, H_2O, rt to reflux; viii) $CeCl_3 \cdot 7H_2O$, $NaBH_4$, MeOH, 0 °C to rt.

Structure-Affinity Studies of NCS-382 Analogs (1a–n) at CaMKIIα. To extend our knowledge of the structure-affinity relationship (SAR) of synthesized NCS-382 analogs **1a**–**n** for native CaMKIIα, their affinities toward the specific binding site in the CaMKIIα hub domain were investigated by displacement of [^{3}H]NCS-382 in rat brain cortical homogenates (Figure 2A–B and Table 1), as previously described.[31,33]

First, we investigated the impact of the position of the substituent in the NCS-382 scaffold on affinity. The 1-bromo analog **1a** (K_i 0.23 μM) exhibited an affinity similar to NCS-382, but introducing a bromine in the 2- (**1b**, K_i 0.050 μM) and 3-position (**1c**, K_i 9.7 μM) of the core structure respectively led to a seven times increase and twenty-nine times decrease in affinity (Figure 2A). A similar trend was observed for the biphenyl compounds (**1h**–**j**), substantiating that the positioning of substituents is a key determinant for affinity (Figure S1). However, no

clear preference for the chemical nature of halogens at the C-2 site was shown, as substitution of bromine (**1b**) for fluorine (**1f**, K_i 0.11 μM), chlorine (**1d**, K_i 0.052 μM) and iodine (**1g**, K_i 0.053 μM) practically resulted in equivalent affinities (Figure S1). In contrast, **1e** (K_i 0.32 μM), comprising a methyl group at C-2, was equi-affine to NCS-382 (Figure 2B). To probe the hydrophobic pocket and enhance affinity as noted above, phenyl, styryl and phenylethyl functionalities possessing extended chain lengths were introduced. This idea was consolidated by the observation that introduction of a styrene in both C-1 (**1k**, K_i 0.029 μM) and C-2 (**1l**, K_i 0.040 μM) positions increased the affinity by ten times compared to that of NCS-382 (Figure 2B). Particularly, **1k** displayed the highest affinity in the developed series. We recently reported that Arg433 situated in the CaMKIIα hub domain shows a plausible halogen bonding interaction with the dichlorophenyl ring of 5-HDC, which seems beneficial to the affinity.[5] This prompted us to synthesize 1-(2,6-dichloro)styryl analog **1m** (K_i 0.11 μM) (Figure S1). Yet, this compound displayed a slight decrease in affinity compared to **1k**. Additionally, introducing more flexibility in **1k** accordingly led to a slight decrease in the affinity of **1n** (K_i 0.056 μM) (Figure S1).

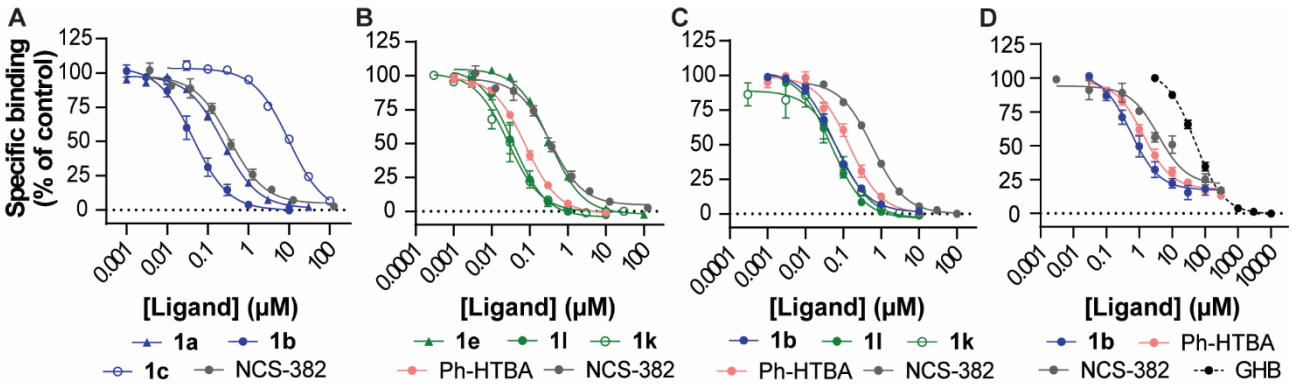

Figure 2. (A–B) Concentration-dependent inhibition of [^{3}H]NCS-382 binding to rat cortical homogenates by (A) **1a**, **1b** and **1c** and (B) **1e**, **1l**, **1k**, and **1i** (Ph-HTBA); NCS-382 for comparison. (C) Inhibition of [^{3}H]HOCPCA binding to rat cortical homogenates by **1b**, **1l**, **1k**, and Ph-HTBA; NCS-382 for comparison. (D) Inhibition of [^{3}H]HOCPCA binding to whole-cell homogenates from HEK293T cells recombinantly expressing CaMKIIα by using **1b**, NCS-

382 and Ph-HTBA; GHB for comparison. Data are presented as normalized means ± SEM from three to five independent experiments performed in technical triplicates. Average K_i values are displayed in Table 1.

Table 1. Collected Binding Affinities of GHB, NCS-382 and Synthesized Analogs 1a–n From Native and Recombinant CaMKIIα Binding Assays[a]

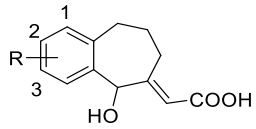

NCS-382 and 1a–n

Compound	R	[^{3}H]NCS-382 binding K_i (μM)[b] [pK_i ± SEM]	[^{3}H]HOCPCA binding K_i (μM) [pK_i ± SEM]	
			native[b]	recombinant[c]
GHB		4.3[d]	3.0[f]	51[f]
NCS-382	H	0.34[e]	0.59 [6.2 ± 0.03]	3.9 [5.4 ± 0.05]
1a	1-Br	0.23 [6.7 ± 0.04]	-	-
1b	2-Br	0.050 [7.4 ± 0.17]	0.057 [7.3 ± 0.06]	0.65 [6.3 ± 0.11]
1c	3-Br	9.7 [5.0 ± 0.09]	-	-
1d	2-Cl	0.052 [7.3 ± 0.02]	-	-
1e	2-Me	0.32 [6.5 ± 0.04]	-	-
1f	2-F	0.11 [7.0 ± 0.05]	-	-
1g	2-I	0.053 [7.3 ± 0.01]	-	-
1h	1-Ph	0.38 [6.4 ± 0.06]	-	-
1i (Ph-HTBA)	2-Ph	0.078 [7.1 ± 0.06]	0.14 [6.9 ± 0.07]	1.4 [5.9 ± 0.15]
1j	3-Ph	14 [4.9 ± 0.15]	-	-
1k	1-PhCHCH	0.029 [7.6 ± 0.13]	0.081 [7.1 ± 0.06]	-
1l	2-PhCHCH	0.040 [7.5 ± 0.13]	0.050 [7.3 ± 0.12]	-
1m	1-(2,6-dichloro)styryl	0.11 [7.0 ± 0.11]	-	-
1n	1-PhCH$_2$CH$_2$	0.056 [7.3 ± 0.07]	-	-

[a]IC_{50} values were calculated from concentration-inhibition curves and converted to corresponding K_i values using the Cheng-Prusoff equation. The data are given as mean K_i along with [mean pK_i ± SEM] values based on the results from three to five independent experiments each performed in technical triplicates. [b]Data were obtained by inhibition of [^{3}H]NCS-382 or [^{3}H]HOCPCA binding to native CaMKIIα in rat cortical homogenates. [c]Data were obtained by inhibition of [^{3}H]HOCPCA binding to whole-cell homogenates from HEK293T cells recombinantly expressing CaMKIIα. [d]From Wellendorph et al., 2005.[31] [e]From Bay et al., 2014.[39] [f]From Leurs et al., 2021.[5] "-" means data not obtained.

To further validate the relatively high affinity of **1b**, **1i** (Ph-HTBA), **1l**, and **1k** towards native CaMKIIα using [^{3}H]NCS-382 as the radioligand, their ability to inhibit the radioligand [^{3}H]HOCPCA was also investigated (Figure 2C and Table 1), using otherwise the exact same binding protocol.[35] As for [^{3}H]NCS-382, analogs **1b**, **1k**, **1l**, and Ph-HTBA displaced [^{3}H]HOCPCA in a concentration-dependent manner and yielded the same overall rank order of affinity (NCS-382>Ph-HTBA>**1b=1l=1k**). Although there was a tendency for a slight loss in affinity in competing with [^{3}H]HOCPCA over [^{3}H]NCS-382, overall similar K_i values were obtained for the mentioned NCS-382 analogs, showing four to twelve times higher affinity than NCS-382 itself.

Finally, to verify the binding of **1b** and Ph-HTBA to recombinant full-length CaMKIIα protein, the [^{3}H]HOCPCA radioligand binding assay was performed using **1b** and Ph-HTBA in whole-cell homogenates prepared from HEK293T cells 48-hours post-transfection with CaMKIIα plasmid (Figure 2D and Table 1). Although it has been reported that this method is less sensitive than the native binding protocol,[5] Ph-HTBA and **1b** still showed three and six times increased affinity compared to NCS-382, and 36 and 78 times improved affinity compared to GHB, respectively. Notably, for NCS-382 and derivatives thereof, we furthermore observed a maximum inhibition (plateau) around 20% in contrast to GHB which completely displaced [^{3}H]HOCPCA. This could indicate that binding of the smaller ligands, HOCPCA and GHB, involves a subpocket partially unavailable to the larger ligands as a function of conformational changes during increased ligand occupancy. The relatively decreased affinities at recombinant CaMKIIα protein compared to native CaMKII may relate to the fact that CaMKIIα, when heterologously expressed in HEK293T cells, is predominantly cytosolic and homomeric.[45-47] This is in contrast to the native membrane-located and presumably heteromeric form of CaMKII in cortical homogenates. Consequently, in a recombinant setting, a

precipitation step is necessary before the filtration which may in itself affect the binding equilibrium.

Altogether, we systematically studied the SAR of fourteen synthesized NCS-382 analogs (**1a**–**n**) in terms of the position, chemical nature, and linker length of different substituents to unravel key determinants for molecular recognition of the NCS-382 scaffold toward the CaMKIIα hub domain binding site. This finding clearly demonstrates a pronounced impact on affinity by targeting a hydrophobic pocket in the upper site of GHB binding site. In addition, three different radioligand binding assays using either native or recombinant CaMKIIα further confirmed enhanced affinities of **1b**, **1l**, **1k**, and Ph-HTBA relative to NCS-382 and GHB, emphasizing them as new high-affinity ligands to selectively target the CaMKIIα hub domain.

Structure-Based Rationalization of SAR Observations at CaMKIIα. To rationalize the molecular basis for the SAR observations, *in silico* docking studies of **1a**–**n** by using the CaMKIIα/5-HDC co-crystal (PDB: 7REC)[5] were conducted. Introduction of a bromine (**1a**) or a phenyl ring (**1h**) in the C-1 position did not lead to additional interactions with the target protein (Figure 3A–B). On the other hand, extending the phenyl ring to reach higher up in the pocket with either a flexible (**1n**) or constrained linker (**1k**) showed a substantial increase in affinity over **1h** and NCS-382. This might be due to the ability to fill out a hydrophobic cavity higher up in the pocket, where the extended phenyl ring could interact with hydrophobic amino acids contouring the pocket: Leu402, Val475, Ile 361, and Val410 with proximal fit (Figure 3C).

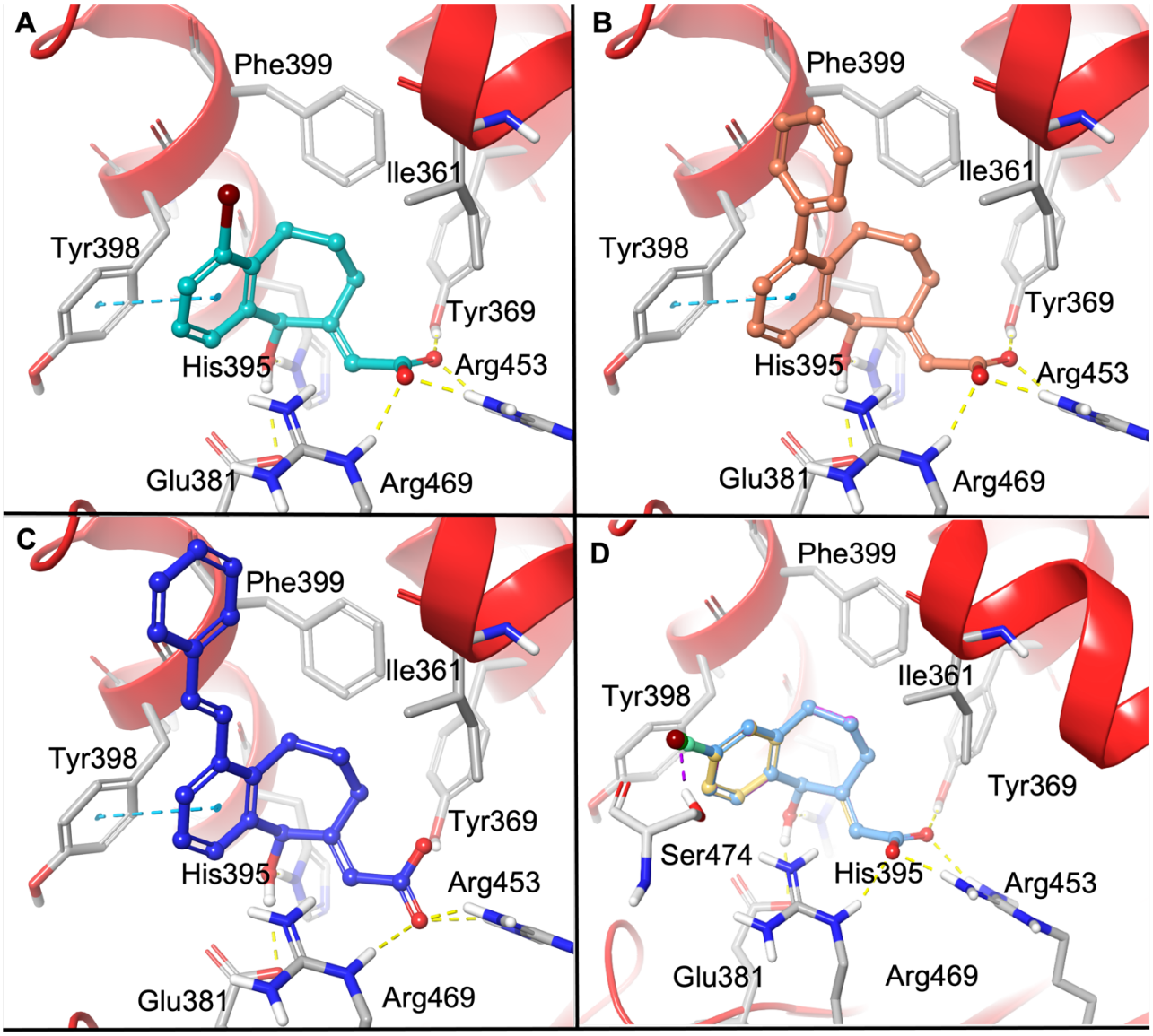

Figure 3. Docking poses for (A) **1a** (cyan), (B) **1h** (orange), and (C) **1k** (blue), and (D) overlaid poses of **1f** (F – light blue), **1d** (Cl – gold), **1b** (Br – magenta), and **1g** (I – light green) in the binding pocket of the CaMKIIα hub domain. Backbone – red, amino acids – gray, aromatic interactions are depicted in cyan dashed lines and hydrogen bonds in dashed yellow lines. The perpendicular side-on halogen/hydrogen-bond donor interaction between the lone electron pair of a halogen atom and Ser474 is depicted in dashed purple line.

Furthermore, the halogenated compounds **1b**, **1d**, and **1g** in the C-2 position showed a pronounced increase in affinity compared to NCS-382. Docking showed that this might be due

to a potential perpendicular, side-on halogen/hydrogen-bond donor interaction between the lone electron pairs of the halogen atoms in **1b**, **1d**, and **1g** and the polar residue Ser474 in the binding cavity (Figure 3D).[48,49] This notion is further supported by the difference in affinity of those ligands compared to **1f** and **1e**, where a fluorine atom or a methyl group was introduced in the corresponding position, respectively. A fluorine atom is as small as a hydrogen atom and has a strong electron-withdrawing effect, therefore might not be able to present same strong interaction with Ser474, resulting in a justified reduction in affinity of **1f**. In addition, a methyl group cannot altogether engage in a halogen/hydrogen-bond donor interaction with Ser474, evidenced by the observation that compound **1e** displayed an even lower affinity than **1f**, while maintaining a similar affinity as NCS-382 itself. Together, this points out a very plausible halogen/hydrogen-bonding interaction between **1b**, **1d**, **1g** and Ser474, resulting in higher affinity than NCS-382, **1f**, and **1e**.

The C-2 phenyl substituted analog, Ph-HTBA, displayed a slightly different binding mode compared to analogs with small substituents in the corresponding position. Ph-HTBA was found to reach the upper hydrophobic cavity by adapting a slightly tilted binding mode, where the introduced phenyl ring at C-2 faces upwards into the hydrophobic cavity (Figure 6A). As a result, Ph-HTBA and the extended analogs, **1k**, **1l**, and **1n**, maintain essential hydrophobic contacts with residues in the hydrophobic pocket (Tyr398 and Phe399) as well as essential core-scaffold polar interactions with His395, Tyr369, Arg453, and Arg469 similar to NCS-382. The aforementioned residues, His395, Tyr398 and Phe399, are part of the helix αD involved in lateral stabilization of the oligomeric complex,[30] whereas the charged arginine residues are known to make the hub domain highly solvated to flexibly accommodate changes in shape, e.g. ligand binding.[28]

Finally, docking studies showed an extremely tight fit and limited space around the C-3 position. Consequently, the C-3 substituted analogs, **1c** and **1j**, showed a substantial decrease

in binding affinity, regardless of the size or nature of introduced group. Together, this confirms that the C-3 position is not accessible for future ligand design.

Assessment of Selected Analogs in an In-House CaMKIIα Biophysical Assay Panel. To enable a consistent characterization of GHB analogs interacting with the CaMKIIα hub domain, we have established a biophysical assay panel for CaMKIIα (Figure 4A), comprising surface plasmon resonance (SPR) binding, differential scanning fluorimetry (DSF) to assess thermal shifts, and intrinsic tryptophan fluorescence (ITF) measurements targeted at the Trp403 positioned in the hub upper cavity.[5] All recombinant proteins were produced in-house. Whereas the SPR and ITF assays utilized the recombinant purified human CaMKIIα 6x hub, the DSF assay used wild-type hub domain instead as the stabilized nature of 6x hub prevents functionality of this assay (T_m > 100 °C). We have previously shown that binding of GHB ligands to CaMKIIα in SPR/ITF is unchanged between 6x and wild-type hub proteins.[5] Since **1b** and Ph-HTBA showed improved affinity toward CaMKIIα compared to NCS-382, these compounds were included for testing in the assays, and additionally, compound **1k** was included in the Trp403 flip assay owing to the extended length of the styryl group.

Real-time interaction studies of compounds binding to the CaMKIIα hub by SPR revealed increases in binding affinity for both **1b** and Ph-HTBA (K_D of 2.6 μM and 757 nM, respectively) compared to NCS-382 (K_D of 8.9 μM) (Figure 4B–D). Furthermore, a change in the kinetic profile was observed, particularly for Ph-HTBA, having a 25-fold slower dissociation rate (k_d of 0.03 s^{-1}) than NCS-382 (k_d of 0.75 s^{-1}) (Figure S2, Table S1).

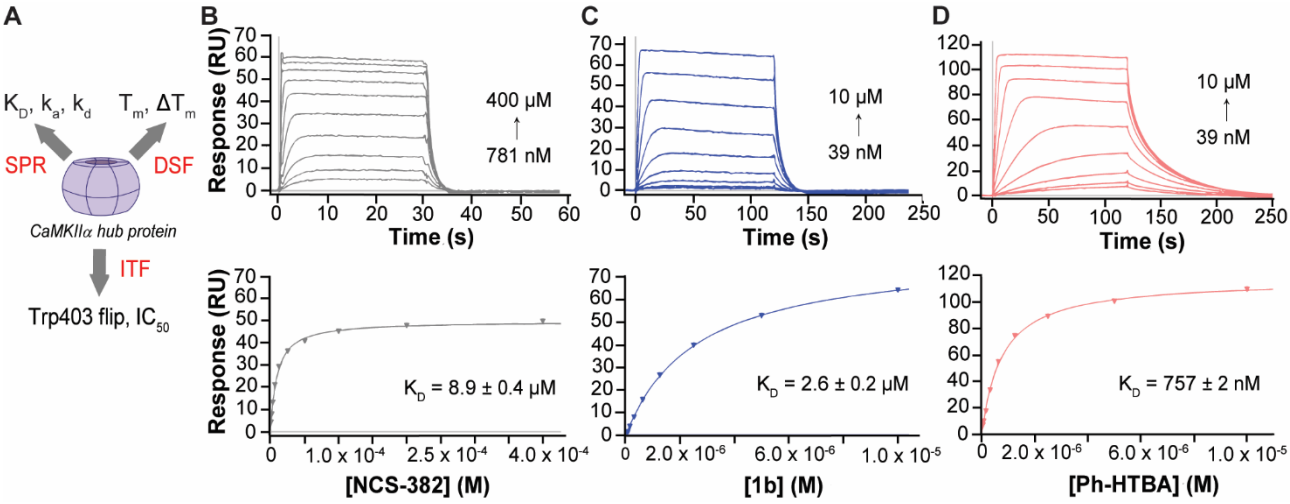

Figure 4. (A) Biophysical assay panel of the CaMKIIα hub domain and associated pharmacological parameters. (B–D) SPR interactions of (B) NCS-382, (C) **1b** and (D) Ph-HTBA to CaMKIIα 6x hub. Compounds in two-fold dilution series were injected in order of increasing concentration over the biosensor surface with immobilized CaMKIIα 6x hub. *Upper*, sensorgrams. *Lower*, plots of equilibrium binding responses fitted to a 1:1 binding model.

As major stabilization effects of the oligomeric CaMKIIα hub protein upon binding of GHB analogs have previously been detected,[5] we also measured the thermal shift induced by NCS-382 analogs (**1b** and Ph-HTBA) using DSF. As expected, we observed a large concentration-dependent stabilizing effect of the CaMKIIα hub oligomer by NCS-382, **1b**, and Ph-HTBA**,** resulting in maximum ΔT_m of 16.7, 17, and 19 °C, respectively (Figure 5A–C and S3). These findings are in line with previous studies with other GHB analogs (5-HDC, GHB, and HOCPCA), which have all been reported to right-shift the protein melting curves, underlining the common role of GHB analogs in stabilizing hub oligomeric states upon binding.[5] Notably, compared to NCS-382 and **1b**, Ph-HTBA displayed the most pronounced thermal shift when comparing the concentrations needed to generate maximum ΔT_m. Although further studies are needed to clarify these findings, it suggests that these compounds promote a lateral stabilization

by reducing the release of dimers, possibly by reorientation of the helix αD.[30] This may also relate to the ability of the compounds to interact with centrally located arginine residues in the highly solvated hub cavity to neutralize local charges.[28] The fact that Ph-HTBA, the larger-sized ligand, has larger T_m shifts than **1b** and NCS-382 may be due to stronger molecular interactions with residues in the helix αD (Figure 6A), increasing the energy required to unfold the protein, but may also merely relate to differences in kinetics as Ph-HTBA has a slower off-rate (Figure 4 and S2).

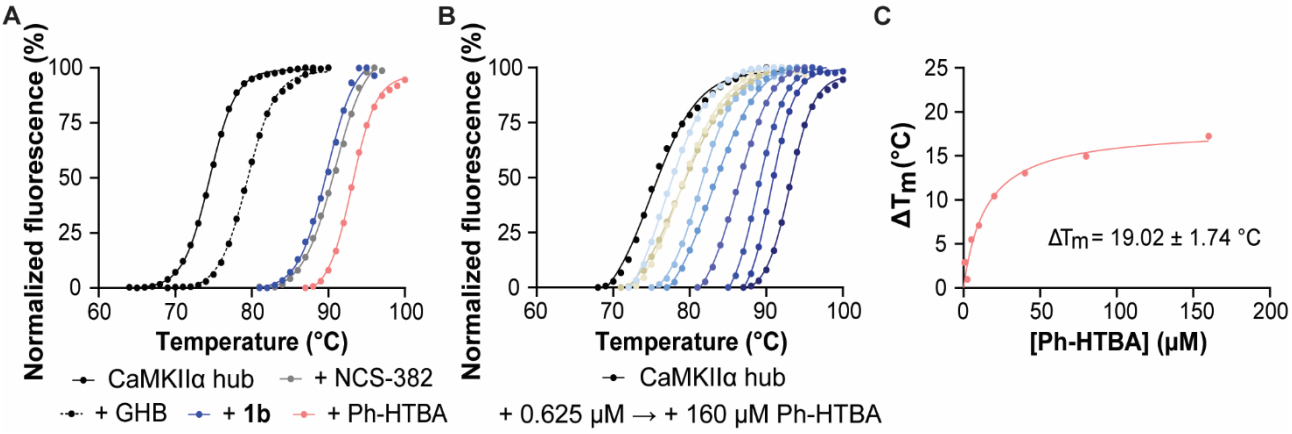

Figure 5. Thermal shift of the CaMKIIα wild-type hub domain protein assessed by DSF. (A) Right-shifted melting curves by GHB,[5] NCS-382 (1280 µM), **1b** (320 µM), and Ph-HTBA (160 µM) in saturating concentrations. (B) Concentration-dependent right-shift of Ph-HTBA, and (C) corresponding saturation isotherm deriving maximum ΔT_m when fitted to a 1:1 model. Representative data of three to four independent experiments.

Finally, to assess actual movement of Trp403 out of the binding cavity (flip out) upon compound binding, docking was performed for Ph-HTBA (Figure 6A) predicting such an event to occur. Then, to probe experimentally, ITF was measured using quenching of the Trp403 upon movement, as reported earlier.[5] In this assay, NCS-382 caused no apparent change in fluorescence in high micromolar concentrations compared to the hub domain alone, no

background fluorescence and no internal absorbance at the tested concentration (Figure 6B). By contrast, Ph-HTBA displayed background fluorescence, some internal absorbance at high concentrations, and fluorescent quenching, obscuring straightforward analysis (Figure 6C). Thus, to fully profile Ph-HTBA, we examined its concentration-dependent relationship and carefully corrected for compound-related interfering spectral properties. This resulted in a concentration-dependent inhibition of the ITF with an IC_{50} value of 452 μM (Figure 6D). This is far from the potency measured for 5-HDC (IC_{50} 1.81 μM) using the same assay,[5] possibly ascribed both to the differences in binding affinity between Ph-HTBA and 5-HDC, and the aforementioned interfering effects on emission wavelength. To further ascertain whether compounds containing bulky aromatic substituents cause significant Trp403 flip to measure, we also tested compound **1k** in two independent runs. As shown in Figure S4, **1k** was likewise able to cause a Trp flip, however, no full concentration-dependent curve could be generated. Altogether, it is concluded that **1k** and Ph-HTBA induced a molecular displacement of Trp403 upon binding which was large enough to consistently measure. This correlates well with the docking models of these two compounds reaching up into the hydrophobic space in the upper cavity of the hub (Figure 3C and 6A) and the physical displacement of Trp403 when they are bound in the pocket.

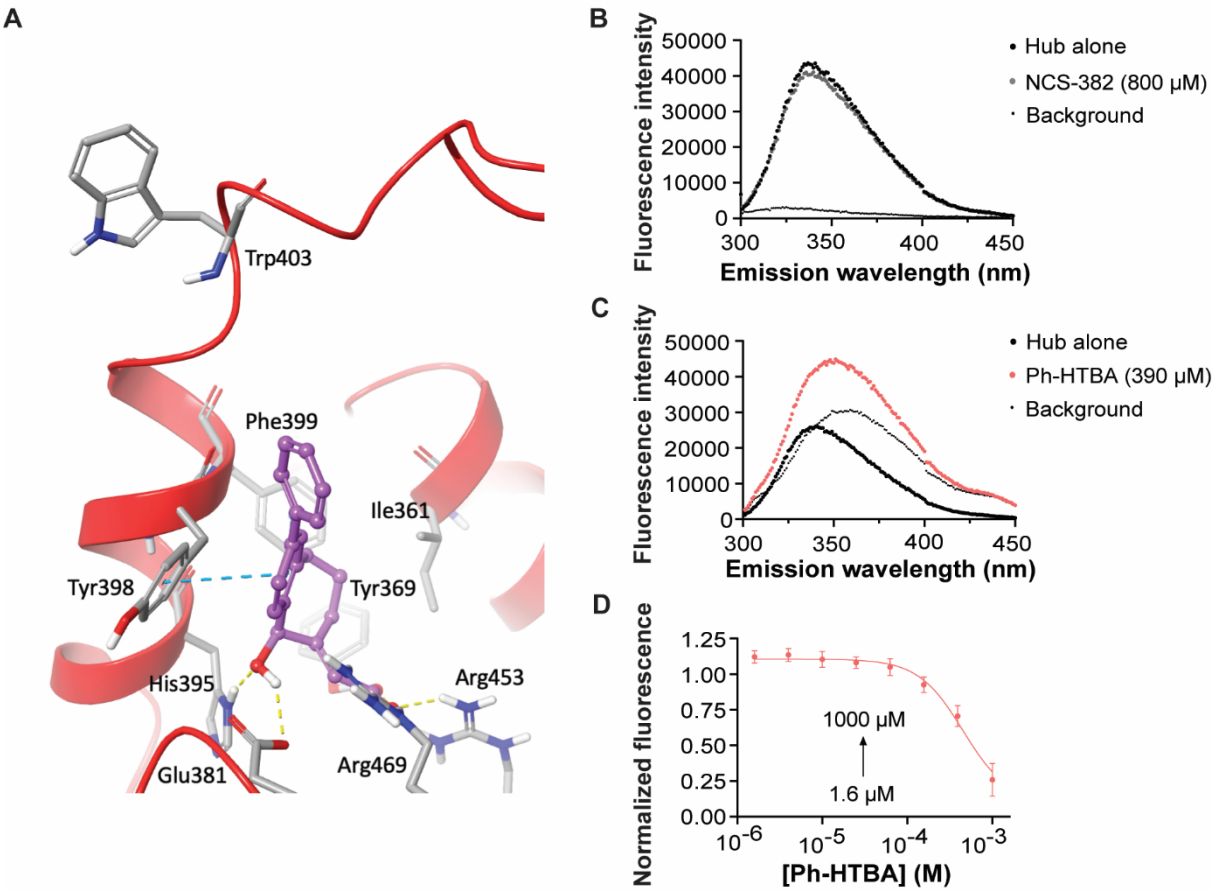

Figure 6. (A) Proposed binding mode of Ph-HTBA (purple) in the binding pocket of the CaMKIIα hub domain, with clear Trp403 flip outward. Backbone – red, amino acids – gray, aromatic interactions are depicted in cyan dashed lines and hydrogen bonds in dashed yellow lines. (B–C) Quenching of ITF caused by Trp403 flip in the CaMKIIα 6x hub domain protein upon compound interaction of (B) NCS-382 and (C) Ph-HTBA; representative data. (D) Concentration-dependent inhibition curve of Ph-HTBA, pooled data (n = 5, mean ± SEM). Background refers to the compound in buffer alone.

In terms of the observed thermal stabilization offered particularly by the larger-sized ligands typified by Ph-HTBA, it is noteworthy that the Trp403 residue is found close to the helix αD and may thus contribute further to the lateral stabilizing effects of the hub oligomeric complex *via* its movement. All in all, the stabilizing effect of Ph-HTBA may involve a cumulative number of molecular events including both its specific binding pocket reaching high up into

the cavity, a high affinity, slow dissociation kinetics, and the observed Trp403 flip. These characteristics underscore Ph-HTBA as a unique representative in the newly developed NCS-382 series which is also chemically feasible to be synthesized in gram-scale *via* a cost-effective approach (Scheme 1). Accordingly, we decided to use Ph-HTBA for further pharmacokinetic evaluations.

Pharmacokinetic Assessment. In 2016, Ainslie et al.[50] reported a short half-life of NCS-382 in mice (0.3 h in serum after intraperitoneal administration), with fast and total elimination occurring primarily *via* hepatic metabolism. Further, glucuronidation of NCS-382, occurring *via* UDP glucuronosyltransferase family 2 member B7 (UGT2B7), proved to be a principal metabolic pathway.[50] Inspired by Ainslie's work, the metabolic fate of Ph-HTBA was evaluated *in vitro* in mouse and human liver microsomes and hepatocytes, and *in vivo* in C57BL6/J mice. Particularly, aiming to improve the solubility of this compound in aqueous media, the sodium salt of Ph-HTBA was prepared by neutralization of the carboxylic acid moiety of Ph-HTBA with sodium hydroxide and utilized for subsequent pharmacokinetic investigations. In mouse preparations, Ph-HTBA showed low clearance in liver microsomes but high hepatic clearance, whereas in human preparations, both values were low (Table 2). To further evaluate total intrinsic clearance *in vivo*, the sodium salt of Ph-HTBA was intravenously injected to mice at a dose of 1 mg/kg. In accordance with the obtained *in vitro* results of Ph-HTBA and the reported *in vivo* metabolism of NCS-382[50] in mice, Ph-HTBA showed a rapid elimination from plasma after intravenous administration, indicating an overall high *in vivo* clearance in mice (Figure S5).

Table 2. Metabolic Fate of Ph-HTBA in Mouse and Human Liver Microsomes and Hepatocytes[a]

Compound	Liver microsomal clearance CL_i (μL/min/mg protein)		Hepatic clearance CL_i (μL/min/10^6 cell)	
	Mouse	Human	Mouse	Human
Ph-HTBA	<9.9	<9.9	65	8.6

[a]The metabolic stability of Ph-HTBA was examined by using the Ph-HTBA sodium salt (0.5 μM) in mouse and human liver microsomes at 0.5 mg/mL protein concentration, and in hepatocytes at the cell concentration of 0.5 x 10^6 cells/mL. The intrinsic clearance (CLi) data are given as the mean values obtained from two independent experiments.

Next, in order to verify the brain permeability profile for Ph-HTBA, we assessed its total brain exposure after oral administration. The Ph-HTBA sodium salt was administered to C57BL6/J mice at a dose of 10 mg/kg and the brain-to-plasma distribution was evaluated. The measured brain and plasma concentrations of Ph-HTBA were 99.1 ng/mL and 1450 ng/mL, respectively, resulting in a brain-plasma ratio of 0.10 and an unbound partition coefficient (Kp, uu) value of 0.85. Whereas a low plasma concentration of Ph-HTBA after oral administration demonstrates its low bioavailability in mice, the obtained high Kp, uu value indicates good brain permeability for Ph-HTBA.

We also assessed the cellular permeability using MDCKII cells expressing either multidrug resistance mutation (MDR-1) (i.e. P-glycoprotein; P-gp) or breast cancer resistance protein (BCRP) (Table 3). Ph-HTBA was found to display good cellular permeability, giving high apparent permeability coefficients (Papp) but low efflux ratios (close to 1). Since efflux transporters for P-gp and BCRP have been reported to cooperatively restrict the entry and promote efflux of drug candidates in the brain and have in fact proved to adversely affect the total brain exposure of GHB analogs,[6, 51] it was important to note that Ph-HTBA was neither a substrate of P-gp nor the BCRP transporter. This is consolidated with the unchanged Papp values and efflux ratios obtained in the absence or presence of elacridar (P-gp transporter

inhibitor) in MDCKII MDR1 cells and Ko 143 (BCRP transporter inhibitor) in MDCKII BCRP cells.

Table 3. Permeability Data of Ph-HTBA in MDCKII BCRP Cells and MDCKII MDR1 Cells[a]

Direction ± inhibitor	MDCKII BCRP cells		MDCKII MDR1 cells	
	mean Papp (nm/sec)	efflux ratio	mean Papp (nm/sec)	efflux ratio
A→B	158	-	130	-
B→A	194	1.2	163	1.3
A→B + Ko 143	159	-	-	-
B→A + Ko 143	165	1.0	-	-
A→B + elacridar	-	-	129	-
B→A + elacridar	-	-	150	1.2

[a]The permeability of Ph-HTBA in MDCKII BCRP and MDR1 cells was measured in two directions: apical to basolateral (A→B) and basolateral to apical (B→A) in the presence or absence of inhibitors. Each experiment was performed in triplicate sets of wells. Ko 143 is a potent and selective inhibitor for BCRP efflux transporter, while elacridar is a dual inhibitor for P-gp and BCRP efflux transporters. A test item is considered as an efflux transporter substrate when the efflux ratio is >2 in the absence of an inhibitor and significantly reduced in the presence of an inhibitor. "-" means not tested.

Conclusion

In summary, guided by *in silico* studies using the CaMKIIα/5-HDC crystal structure, we synthesized a series of new NCS-382 analogs (**1a**–**n**) to dissect structural determinants of this chemical scaffold for molecular recognition of the CaMKIIα hub domain binding site. Through systematic SAR exploration, this study highlights a pronounced impact on affinity by employing non-polar aromatic substituents to target a hydrophobic pocket in the upper part of the binding pocket, resulting in three to twelve times increased affinity compared to NCS-382. Particularly, Ph-HTBA (**1i**), the C-2 phenyl substituted analog, was further certified as a new mid-nanomolar-affinity ligand for CaMKIIα and found to confer a marked thermal stabilization of the hub oligomer along with a distinct structural movement of Trp403 upon binding. Furthermore, Ph-HTBA not only exhibited good cellular permeability, but also, importantly,

proved to be brain-penetrant after systemic administration to mice, signified by a high Kp,uu value. Altogether, this emphasizes Ph-HTBA as an important and emerging compound for further *in vitro* and *in vivo* CaMKII neuropharmacological interventions. Given that this compound can be feasibly prepared in gram-scale and its sodium salt displays good aqueous solubility, Ph-HTBA thus represents a potential substance for future clinical development as well.

Experimental Section

Chemistry. *General Procedure.* All reagents and solvents (reagent or chromatography grade) were purchased and used without further purification unless specified. Air- and/or moisture-sensitive reactions were performed under the protection of argon or nitrogen gas using syringe-septum techniques, and glassware was dried by flame or using an oven. Anhydrous solvents were prepared by using a solvent purification system (DMF and THF) or by storage over 3 Å or 4 Å molecular sieves. Thin layer chromatography (TLC) was carried out using Merck silica gel 60 F_{254} plates, and it was visualized *via* UV light (254 nm) and a $KMnO_4$ spray reagent. Flash column (FC) chromatography was carried out by using Merck Geduran® silica gel 60 (0.040-0.063 mm).

The ^{1}H or ^{13}C NMR spectra were recorded on a Bruker Advance 400MHz spectrometer assembled with a 5 mm BBFO probe or a Bruker Advance 600 MHz spectrometer with a cryogenically cooled 5 mm $^{13}C/^{1}H$ DCH probe at 300 K. The data were tabulated in the following order: chemical shift (δ) [multiplicity (b, broad; s, singlet; d, doublet; t, triplet; q, quartet; m, multiplet), coupling constant(s) *J* (Hz), number of protons]. The solvents used for NMR were chloroform-*d* (reference signals δ_H = 7.26 ppm and δ_C = 77.16 ppm), methanol-d_4 (reference signals δ_H = 3.31 ppm and δ_C = 49.00 ppm) or DMSO-d_6 (reference signals δ_H =

2.50 ppm and δ_C = 39.52 ppm). The solvent residue peak or trimethylsilane was used as internal reference.

Ultraperformance liquid chromatography–mass spectroscopy (UPLC-MS) analysis was carried out on a Waters Acquity H-class UPLC using a Sample Manager FTN and a TUV dual wavelength detector coupled to a QDa single-quadrupole analyzer using electrospray ionization. UPLC separation was achieved using a C18 reversed-phase column (Acquity UPLC BEH C18, 2.1 mm × 50 mm, 1.7 μm) operated at 40 °C, using a linear gradient of the binary solvent system of buffer A (Milli-Q H_2O/MeCN/formic acid, 95:5:0.1 v/v%) to buffer B (MeCN/formic acid, 100:0.1 v/v%) from 0 to 100% B in 3.5 min and then 1 min at 100% B, maintaining a flow rate of 0.8 mL/min. Data acquisition was controlled by MassLynx ver. 4.1, and data analysis was done using Waters OpenLynx browser ver. 4.1.

Purity was assessed by analytical high-performance liquid chromatography (HPLC) performed on an UltiMate HPLC system (Thermo Scientific) comprising an LPG-3400A pump, a WPS-3000SL auto-sampler, and a DAD-3000D diode array detector (254 nm), using a Gemini-NX C18 column (4.6 × 250 mm, 3 μm, 110 Å) (Phenomenex). A linear gradient elution was utilized with eluent A (Milli-Q H_2O/TFA, 100:0.1 v/v%) containing 0% of eluent B (MeCN/Milli-Q H_2O/TFA, 90:10:0.1 v/v%) rising to 100% of B within 15 minutes at a stable flow rate of 1.0 mL/min. The data were acquired and processed using Chromeleon Software ver. 6.80. The purities of the analyzed compounds were ≥95%, unless otherwise stated.

Preparative reverse-phase HPLC was performed on an UltiMate HPLC system (Thermo Scientific) consisting of an HPG-3200BX pump, a Rheodyne 9725i injector, a 10 mL loop, an MWD-3000SD detector (254nm), and an AFC-3000SD automated fraction collector using a Gemini-NX C18 column (21.2 × 250 mm, 5 μm, 110 Å) (Phenomenex). Mobile phases A (Milli-Q H_2O/TFA 100:0.1 v/v%) and B (MeCN/Milli-Q H_2O/TFA 90:10:0.1 v/v%) with a

flow rate of 20 mL/min were applied. For HPLC control, data collection and data handling, Chromeleon software ver. 6.80 was used.

General Procedure A for Luche Reduction. $CeCl_3 \cdot 7H_2O$ (1.1 equiv) and compound **6a**–**n** (1 equiv) were dissolved in MeOH. $NaBH_4$ (3–20 equiv) was slowly added to the solution at 0 °C. The reaction was stirred at room temperature for 4h and then solvent was evaporated *in vacuo*. Water was added to the residue and the pH was adjusted to 1 with 2N HCl. The aqueous phase was extracted with EtOAc. The combined organic phases were dried over Na_2SO_4, filtered, and evaporated *in vacuo* to dryness. Purification using FC chromatography provided the desired products **1a**–**n**.

General Procedure B for Witting Condensation. To a solution of (3-carboxypropyl)-triphenylphosphonium bromide (1.1 equiv) in anhydrous THF was added dropwise a solution of sodium bis(trimethylsilyl) amide (2.2 equiv, 1.0 M in THF) at 0 °C under a nitrogen atmosphere. The solution was stirred for 30 minutes at 0 °C and then cooled to -78 °C. Benzaldehyde **2a**–**e**, **i** (1 equiv) was added dropwise. The reaction was allowed to warm to room temperature overnight. Water and diethyl ether were added. The aqueous layer was separated and acidified with 1N aqueous HCl to pH=1, then extracted with EtOAc. The combined organic phases were dried over Na_2SO_4, filtered, and evaporated *in vacuo* to dryness. Purification using FC chromatography provided the desired products **3a**–**e**, **i**.

General Procedure C for Hydrogenation. To a solution of the alkene **3a**–**e**, **i** and **5k** (1 equiv) in EtOAc, Pd/C (10% w/w% loading) was added. The reaction was stirred under a hydrogen atmosphere overnight and then filtered over a short pad of celite. Upon evaporation *in vacuo* to dryness, crude products **4a**–**e**, **i** and **5n** were used directly for the next step without purification.

General Procedure D for Intramolecular Cyclization. A mixture of 5-phenylpentanoic acid **4a**–**e**, **i** (1 equiv) and polyphosphoric acid (15-60 equiv) was stirred at 100 ºC or 130 ºC

under an argon atmosphere. After 2 hours, the reaction mixture was cooled to 100 ºC before a solution of 2N NaOH was added until pH=7. After cooling at room temperature, the solution was extracted with CH_2Cl_2, dried over Na_2SO_4, filtered, and evaporated *in vacuo* to dryness. Purification using FC chromatography provided the desired products **5a**–**e**, **i**.

General Procedure E for Suzuki–Miyaura Cross-Coupling. Phenylboronic acid (2 equiv) and K_2CO_3 (3 equiv) were added to a solution of bromo-6,7,8,9-tetrahydro-5*H*-benzo[7]annulen-5-one **5a**–**c** (1 equiv) in DMF and water. The solution was degassed under a stream of nitrogen for 10 min, then tetrakis(triphenylphosphine)palladium (0.1 equiv) was added and the mixture was degassed under a flow of nitrogen for additional 10 minutes. The reaction was heated at reflux for 24 hours. After cooling to room temperature, water was added and the mixture was extracted with diethyl ether. The combined organic phases were washed with brine, dried over Na_2SO_4, filtered, and evaporated *in vacuo* to dryness. Purification using FC chromatography provided the desired products **5h**–**j**.

General Procedure F for Heck Cross-coupling. Under a nitrogen atmosphere, bromo-6,7,8,9-tetrahydro-5*H*-benzo[7]annulen-5-one **5a**–**b** (1 equiv), corresponding styrene (2 equiv) were dissolved in anhydrous DMF. To this solution were added $Pd(OAc)_2$ (0.1 equiv), PPh_3 (0.2 equiv) and K_2CO_3 (2 equiv). The solution was degassed under a stream of nitrogen for approximately 0.5 h prior to heating at 110 °C for 5h. After cooling to room temperature, the solution was filtered over a short pad of celite and the celite was washed with EtOAc. The organic phase was washed with brine, dried over Na_2SO_4, filtered, and evaporated *in vacuo* to dryness. Purification using FC chromatography provided the desired products **5k**–**m**.

General Procedure G for Claisen–Schmidt Condensation. To a solution of NaOH (6 equiv) in water was added a mixture of compound **5a**–**n** (1 equiv) and glyoxylic acid monohydrate (4 equiv) in ethanol at room temperature. The mixture was stirred at room temperature until dissolution and then heated at reflux for 4h. After cooling, ethanol was

removed *in vacuo*. The residual aqueous solution was washed with diethyl ether and the pH of aqueous phase was adjusted to 1 with 2N HCl and extracted with EtOAc. The combined organic phases were dried over Na_2SO_4, filtered, and evaporated *in vacuo* to dryness. Purification using FC chromatography provided the desired products **6a**–**n**.

(*E*)-2-(1-Bromo-5-hydroxy-5,7,8,9-tetrahydro-6*H*-benzo[7]annulen-6-ylidene)acetic acid (1a). The compound **1a** was prepared from **6a** (0.17 g, 0.56 mmol)**,** $CeCl_3 \cdot 7H_2O$ (0.24 g, 0.62 mmol), $NaBH_4$ (0.21 g, 5.6 mmol) and MeOH (8 mL), using general procedure A. Purification by FC chromatography (CH_2Cl_2/MeOH 95:5 + 1% AcOH) yielded **1a** (92 mg, 55%) as a white solid. ^{1}H NMR (400 MHz, Methanol-d_4) δ 7.51 – 7.44 (m, 2H), 7.09 (t, J = 7.8 Hz, 1H), 6.04 (s, 1H), 5.37 (s, 1H), 3.52 – 3.35 (m, 2H), 3.09 – 2.98 (m, 1H), 2.71 – 2.60 (m, 1H), 1.88 – 1.76 (m, 1H), 1.69 – 1.57 (m, 1H). ^{13}C NMR (101 MHz, Methanol-d_4) δ: 170.3, 163.8, 145.0, 139.9, 132.9, 129.0, 126.5, 125.5, 115.8, 77.5, 32.5, 30.8, 27.5. UPLC-MS: m/z calculated $[M-H]^-$ for $C_{13}H_{12}BrO_3$, 295.00; found 295.0. Purity by anal. HPLC: 98% (254 nm).

(*E*)-2-(2-Bromo-5-hydroxy-5,7,8,9-tetrahydro-6*H*-benzo[7]annulen-6-ylidene)acetic acid (1b). The compound **1b** was prepared from **6b** (2.9 g, 9.7 mmol)**,** $CeCl_3 \cdot 7H_2O$ (4.0 g, 10.7 mmol), $NaBH_4$ (5.5 g, 0.15 mol) and MeOH (100 mL), using general procedure A. Purification by FC chromatography (CH_2Cl_2/MeOH 95:5 + 1% AcOH) yielded **1b** (1.9 g, 65%) as a white solid. ^{1}H NMR (600 MHz, Methanol-d_4) δ 7.38 (d, J = 8.2 Hz, 1H), 7.34 (dd, J = 8.2, 2.1 Hz, 1H), 7.26 (d, J = 2.0 Hz, 1H), 6.00 (s, 1H), 5.25 (s, 1H), 3.51 – 3.44 (m, 1H), 3.07 – 3.00 (m, 1H), 2.83 – 2.71 (m, 2H), 1.88 – 1.78 (m, 1H), 1.75 – 1.65 (m, 1H). ^{13}C NMR (151 MHz, Methanol-d_4) δ 170.3, 163.8, 143.8, 141.7, 133.3, 130.5, 128.9, 121.9, 115.7, 77.7, 35.0, 30.9, 29.0. UPLC-MS: m/z calculated $[M-H]^-$ for $C_{13}H_{12}BrO_3$, 295.00; found 295.0. Purity by anal. HPLC: 96% (254 nm).

(*E*)-2-(3-Bromo-5-hydroxy-5,7,8,9-tetrahydro-6*H*-benzo[7]annulen-6-ylidene)acetic acid (1c).

The compound **1c** was prepared from **6c** (0.26 g, 0.87 mmol)**,** $CeCl_3 \cdot 7H_2O$ (0.36 g, 0.95 mmol), $NaBH_4$ (0.33 g, 8.7 mmol) and MeOH (10 mL), using general procedure A. Purification by FC chromatography (CH_2Cl_2/MeOH 95:5 + 1% AcOH) yielded **1c** (0.14 g, 54%) as a white solid. ^{1}H NMR (600 MHz, Methanol-d_4) δ 7.64 (d, J = 2.2 Hz, 1H), 7.28 (dd, J = 8.0, 2.2 Hz, 1H), 7.00 (d, J = 8.0 Hz, 1H), 6.01 (s, 1H), 5.28 (s, 1H), 3.60 – 3.53 (m, 1H), 3.02 – 2.95 (m, 1H), 2.84 – 2.77 (m, 1H), 2.70 – 2.62 (m, 1H), 1.92 – 1.83 (m, 1H), 1.67 – 1.57 (m, 1H). ^{13}C NMR (151 MHz, Methanol-d_4) δ: 170.3, 163.8, 145.0, 140.3, 132.4, 131.2, 129.3, 121.2, 115.6, 77.0, 34.9, 31.5, 29.0. UPLC-MS: m/z calculated [M-H]$^-$ for $C_{13}H_{12}BrO_3$, 295.00; found 295.0. Purity by anal. HPLC: 99% (254 nm).

(*E*)-2-(2-Chloro-5-hydroxy-5,7,8,9-tetrahydro-6*H*-benzo[7]annulen-6-ylidene)acetic acid (1d).

The compound **1d** was prepared from **6d** (0.76 g, 3.0 mmol)**,** $CeCl_3 \cdot 7H_2O$ (1.2 g, 3.3 mmol), $NaBH_4$ (1.1 g, 30.0 mmol) and MeOH (150 mL), using general procedure A. Purification by FC chromatography (CH_2Cl_2/MeOH 95:5 + 1% AcOH) yielded **1d** (0.40 g, 53%) as a white solid. ^{1}H NMR (400 MHz, Methanol-d_4) δ 7.44 (d, J = 8.3 Hz, 1H), 7.19 (dd, J = 8.3, 2.3, 1H), 7.11 (d, J = 2.3 Hz, 1H), 6.00 (s, 1H), 5.27 (s, 1H), 3.49 – 3.45 (m, 1H), 3.07 – 3.02 (m, 1H), 2.81 – 2.73 (m, 2H), 1.86 – 1.80 (m, 1H), 1.74 – 1.68 (m, 1H). ^{13}C NMR (101 MHz, Methanol-d_4) δ 170.3, 164.0, 143.5, 141.2, 133.9, 130.3, 128.7, 127.4, 115.6, 77.8, 35.0, 30.9, 29.0. UPLC-MS: m/z calculated [M-H]$^-$ for $C_{13}H_{12}ClO_3$, 251.05; found 251.2. Purity by anal. HPLC: 95% (254 nm).

(*E*)-2-(5-Hydroxy-2-methyl-5,7,8,9-tetrahydro-6*H*-benzo[7]annulen-6-ylidene)acetic acid (1e). The compound **1e** was prepared from **6e** (3.6 g, 15.5 mmol)**,** $CeCl_3 \cdot 7H_2O$ (6.4 g, 17.0 mmol), $NaBH_4$ (8.8 g, 0.23 mol) and MeOH (150 mL), using general procedure A. Purification by FC chromatography (CH_2Cl_2/MeOH 30:1 + 1% AcOH) followed by recrystallization from EtOAc yielded **1e** (1.6 g, 43%) as a white solid. ^{1}H NMR (400 MHz,

Methanol-d_4) δ 7.29 (d, J = 7.7 Hz, 1H), 7.00 (dd, J = 7.8, 1.9 Hz, 1H), 6.90 (d, J = 1.9 Hz, 1H), 5.96 (s, 1H), 5.22 (s, 1H), 3.40 – 3.33 (m, 1H), 3.12 – 3.01 (m, 1H), 2.87 – 2.79 (m, 1H), 2.76 – 2.69 (m, 1H), 2.27 (s, 3H), 1.83 – 1.71 (m, 2H). ^{13}C NMR (101 MHz, Methanol-d_4) δ 170.4, 164.8, 141.2, 139.1, 138.4, 131.5, 128.1, 127.6, 115.3, 79.0, 35.2, 30.5, 29.4, 21.0. UPLC-MS: m/z calculated [M-H]$^-$ for $C_{14}H_{15}O_3$, 231.10; found 231.4. Purity by anal. HPLC: >99% (254 nm).

(*E*)-2-(2-Fluoro-5-hydroxy-5,7,8,9-tetrahydro-6*H*-benzo[7]annulen-6-ylidene)acetic acid (1f). The compound **1f** was prepared from impure **6f** (0.13 g)**,** $CeCl_3 \cdot 7H_2O$ (0.24 g, 0.64 mmol), $NaBH_4$ (0.22 g, 5.8 mmol) and MeOH (30 mL), using general procedure A. Purification by preparative HPLC (gradient 30−68.5% B, eluent A (Milli-Q H_2O/TFA, 100:0.1) and eluent B (MeCN/ Milli-Q H_2O/TFA, 90:10:0.1) at a flow rate of 20 mL·min^{-1}, over 11 min) yielded **1f** (23 mg, 5% (overall yield calculated based on the applied amount of **5b**)) as a white solid. ^{1}H NMR (600 MHz, Methanol-d_4) δ 7.44 (dd, J = 8.5, 5.9 Hz, 1H), 6.90 (td, J = 8.5, 2.7 Hz, 1H), 6.84 (dd, J = 9.6, 2.7 Hz, 1H), 5.98 (s, 1H), 5.26 (s, 1H), 3.46 – 3.39 (m, 1H), 3.12 – 3.05 (m, 1H), 2.84 – 2.75 (m, 2H), 1.85 – 1.71 (m, 2H). ^{13}C NMR (151 MHz, Methanol-d_4) δ 170.3, 164.2, 163.4 (d, J = 244.2 Hz), 144.1 (d, J = 7.3 Hz), 138.4 (d, J = 2.8 Hz), 129.2 (d, J = 8.3 Hz), 117.2 (d, J = 22 Hz), 115.6, 113.6 (d, J = 21 Hz), 78.1, 35.1, 30.6, 29.0. ^{19}F NMR (376 MHz, Methanol-d_4) δ -118.3. UPLC-MS: m/z calculated [M-H]$^-$ for $C_{13}H_{12}FO_3$, 235.08; found 235.0. Purity by anal. HPLC: 96% (254 nm).

(*E*)-2-(5-Hydroxy-2-iodo-5,7,8,9-tetrahydro-6*H*-benzo[7]annulen-6-ylidene)acetic acid (1g). The compound **1g** was prepared from **6g** (0.15 g, 0.44 mmol)**,** $CeCl_3 \cdot 7H_2O$ (0.16 g, 0.44 mmol), $NaBH_4$ (0.16 g, 4.3 mmol) and MeOH (20 mL), using general procedure A. Purification by preparative HPLC (gradient 30−68.5% B, eluent A (Milli-Q H_2O/TFA, 100:0.1) and eluent B (MeCN/Milli-Q H_2O/TFA, 90:10:0.1) at a flow rate of 20 mL·min^{-1}, over 13 min) yielded **1g** (34 mg, 23%) as a white solid. ^{1}H NMR (600 MHz, Methanol-d_4) δ 7.55 (dd, J = 8.1, 1.9

Hz, 1H), 7.46 (d, *J* = 1.9 Hz, 1H), 7.23 (d, *J* = 8.1 Hz, 1H), 5.99 (s, 1H), 5.24 (s, 1H), 3.50 – 3.45 (m, 1H), 3.04 – 2.98 (m, 1H), 2.80 – 2.71 (m, 2H), 1.86 – 1.79 (m, 1H), 1.73 – 1.65 (m, 1H). ^{13}C NMR (151 MHz, Methanol-d_4) δ 170.3, 163.8, 143.8, 142.4, 139.3, 136.8, 129.0, 115.7, 93.4, 77.8, 34.9, 30.9, 29.0. UPLC-MS: m/z calculated $[M-H]^-$ for $C_{13}H_{12}IO_3$, 342.98; found 343.1. Purity by anal. HPLC: >99% (254 nm).

(*E*)-2-(5-Hydroxy-1-phenyl-5,7,8,9-tetrahydro-6*H*-benzo[7]annulen-6-ylidene)acetic acid (1h). The compound **1h** was prepared from **6h** (0.26 g, 0.88 mmol)**,** $CeCl_3 \cdot 7H_2O$ (0.36 g, 0.97 mmol), $NaBH_4$ (0.34 g, 8.9 mmol) and MeOH (14 mL), using general procedure A. Purification by preparative HPLC (gradient 30−72% B, eluent A (Milli-Q H_2O/TFA, 100:0.1) and eluent B (MeCN/Milli-Q H_2O/TFA, 90:10:0.1) at a flow rate of 20 mL·min^{-1}, over 10 min) yielded **1h** (0.11 g, 40%) as a white solid. ^{1}H NMR (600 MHz, Methanol-d_4) δ 7.50 (d, *J* = 7.7 Hz, 1H), 7.42 – 7.36 (m, 2H), 7.36 – 7.30 (m, 1H), 7.25 – 7.19 (m, 3H), 7.09 (dd, *J* = 7.6, 1.4 Hz, 1H), 6.07 (s, 1H), 5.40 (s, 1H), 3.51 – 3.44 (m, 1H), 3.04 – 2.97 (m, 1H), 2.74 – 2.65 (m, 2H), 1.77 – 1.70 (m, 1H), 1.65 – 1.58 (m, 1H). ^{13}C NMR (151 MHz, Methanol-d_4) δ 170.6, 164.5, 143.6, 143.4, 143.0, 138.3, 130.4, 130.3, 129.1, 127.9, 127.0, 126.3, 115.3, 78.1, 30.9, 29.6, 28.9. UPLC-MS: m/z calculated $[M-H]^-$ for $C_{19}H_{17}O_3$, 293.12; found 293.0. Purity by anal. HPLC: >99% (254 nm).

(*E*)-2-(5-Hydroxy-2-phenyl-5,7,8,9-tetrahydro-6*H*-benzo[7]annulen-6-ylidene)acetic acid (1i, Ph-HTBA). Ph-HTBA (**1i**) was prepared from **6i** (2.4 g, 8.3 mmol)**,** $CeCl_3 \cdot 7H_2O$ (3.4 g, 9.1 mmol), $NaBH_4$ (4.7 g, 0.12 mol) and MeOH (80 mL), using general procedure A. Purification by FC chromatography (CH_2Cl_2 + 1% AcOH) followed by trituration using EtOAc yielded Ph-HTBA (1.7 g, 68%) as a white solid. ^{1}H NMR (600 MHz, Methanol-d_4) δ 7.62 – 7.57 (m, 2H), 7.52 (d, *J* = 7.9 Hz, 1H), 7.45 (dd, *J* = 7.9, 2.0 Hz, 1H), 7.43 – 7.38 (m, 2H), 7.35 (d, *J* = 2.0 Hz, 1H), 7.30 (tt, *J* = 7.4, 1.2 Hz, 1H), 6.02 (s, 1H), 5.33 (s, 1H), 3.50 – 3.43 (m, 1H), 3.20 – 3.13 (m, 1H), 2.91 – 2.80 (m, 2H), 1.90 – 1.75 (m, 2H). ^{13}C NMR (151 MHz,

Methanol-d_4) δ 170.4, 164.6, 142.2, 141.8, 141.7, 141.3, 129.8, 129.3, 128.2, 127.9, 127.9, 126.1, 115.4, 78.6, 35.5, 30.8, 29.4. UPLC-MS: m/z calculated $[M-H]^-$ for $C_{19}H_{17}O_3$, 293.12; found 293.0. Purity by anal. HPLC: >99% (254 nm).

The sodium salt of Ph-HTBA was prepared from Ph-HTBA (1.2 g, 4.0 mmol) by reacting with NaOH (8.0 mL, 4.0 mmol, 0.5M in tritisol) in absolute EtOH (10 mL). The resultant slurry solution at room temperature turned into a clear solution by heating to reflux. After cooling to room temperature, 15 mL of diethyl ether was added to the mixture. The precipitate was filtered off and dried *in vacuo*. The Ph-HTBA sodium salt (1.2 g, 97%) was obtained as an off-white solid. ^{1}H NMR (400 MHz, DMSO-d_6) δ 7.64 – 7.59 (m, 2H), 7.46 – 7.38 (m, 4H), 7.35 – 7.29 (m, 2H), 5.71 (s, 1H), 5.34 (s, 1H), 5.04 (s, 1H), 3.29 – 3.20 (m, 1H), 3.19 – 3.08 (m, 1H), 2.95 – 2.85 (m, 1H), 2.84 – 2.73 (m, 1H), 1.65 – 1.53 (m, 2H). ^{13}C NMR (101 MHz, DMSO-d_6) δ 171.8, 145.5, 143.0, 140.9, 140.2, 138.2, 128.8, 127.6, 127.0, 126.5, 126.2, 125.7, 124.1, 77.2, 34.7, 29.2, 28.0. Elemental analysis: calculated ($C_{19}H_{17}NaO_3 \cdot 0.5H_2O$): C, 70.14; H, 5.58. Found: C, 70.22; H, 5.69. Purity by anal. HPLC: 99% (254 nm).

(*E*)-2-(5-Hydroxy-3-phenyl-5,7,8,9-tetrahydro-6*H*-benzo[7]annulen-6-ylidene) acetic acid (1j). The compound **1j** was prepared from **6j** (84 mg, 0.29 mmol)**,** $CeCl_3 \cdot 7H_2O$ (0.12 g, 0.32 mmol), $NaBH_4$ (55 mg, 1.4 mmol) and MeOH (4 mL), using general procedure A. Purification by FC chromatography (Heptane/EtOAc 7:3 + 1% AcOH) yielded **1j** (63 mg, 73%) as a white solid. ^{1}H NMR (400 MHz, Methanol-d_4) δ 7.73 (d, J = 1.9 Hz, 1H), 7.64 – 7.59 (m, 2H), 7.44 – 7.38 (m, 3H), 7.30 (t, J = 7.4 Hz, 1H), 7.16 (d, J = 7.7 Hz, 1H), 6.05 (s, 1H), 5.36 (s, 1H), 3.54 – 3.43 (m, 1H), 3.17 – 3.06 (m, 1H), 2.89 – 2.75 (m, 2H), 1.92 – 1.70 (m, 2H). ^{13}C NMR (101 MHz, Methanol-d_4) δ 170.4, 164.5, 142.6, 142.3, 140.9, 140.4, 131.3, 129.8, 128.1, 127.8, 126.9, 125.7, 115.5, 78.6, 35.0, 30.9, 29.3. UPLC-MS: m/z calculated $[M-H]^-$ for $C_{19}H_{17}O_3$, 293.12; found 293.2. Purity by anal. HPLC: 99% (254 nm).

(*E*)-2-(5-Hydroxy-1-((*E*)-styryl)-5,7,8,9-tetrahydro-6*H*-benzo[7]annulen-6-ylidene)acetic acid (1k). The compound **1k** was prepared from **6k** (0.10 g, 0.33 mmol), $CeCl_3 \cdot 7H_2O$ (0.14 g, 0.36 mmol), $NaBH_4$ (0.12 g, 3.3 mmol) and MeOH (4 mL), using general procedure A. Purification by preparative HPLC (gradient 30−82.5% B, eluent A (Milli-Q H_2O/TFA, 100:0.1) and eluent B (MeCN/Milli-Q H_2O/TFA, 90:10:0.1) at a flow rate of 20 $mL \cdot min^{-1}$, over 10 min) yielded **1k** (14 mg, 20%) as a white solid. ^{1}H NMR (400 MHz, Methanol-d_4) δ 7.56 – 7.45 (m, 4H), 7.43 (d, J = 7.5 Hz, 1H), 7.34 (t, J = 7.7 Hz, 2H), 7.27 – 7.19 (m, 2H), 6.90 (d, J = 16.1 Hz, 1H), 6.07 (s, 1H), 5.38 (s, 1H), 3.49 – 3.41 (m, 1H), 3.30 – 3.21 (m, 1H), 2.97 – 2.89 (m, 1H), 2.71 – 2.63 (m, 1H), 1.91 – 1.80 (m, 1H), 1.78 – 1.69 (m, 1H). ^{13}C NMR (101 MHz, Methanol-d_4) δ 170.5, 164.7, 142.9, 139.0, 138.6, 137.8, 132.7, 129.7, 128.6, 128.1, 127.6, 127.5, 127.2, 126.8, 115.3, 77.8, 30.6, 28.3, 28.1. UPLC-MS: m/z calculated $[M-H]^-$ for $C_{21}H_{19}O_3$, 319.13; found 318.9. Purity by anal. HPLC: 98% (254 nm).

(*E*)-2-(5-Hydroxy-2-((*E*)-styryl)-5,7,8,9-tetrahydro-6H-benzo[7]annulen-6-ylidene)acetic acid (1l). The compound **1l** was prepared from **6l** (0.12 g, 0.38 mmol), $CeCl_3 \cdot 7H_2O$ (0.16 g, 0.41 mmol), $NaBH_4$ (0.14 g, 3.8 mmol) and MeOH (4 mL), using general procedure A. Purification by FC chromatography (CH_2Cl_2 + 1% AcOH) yielded **1l** (56 mg, 46%) as a white solid. ^{1}H NMR (600 MHz, Methanol-d_4) δ 7.53 (d, J = 6.9 Hz, 2H), 7.45 – 7.37 (m, 2H), 7.36 – 7.30 (m, 3H), 7.23 (tt, J = 7.4, 1.3 Hz, 1H), 7.25 – 7.19 (m, 2H), 6.01 (s, 1H), 5.29 (s, 1H), 3.46 – 3.42 (m, 1H), 3.15 – 3.10 (m, 1H), 2.85 – 2.80 (m, 2H), 1.84 – 1.76 (m, 2H). ^{13}C NMR (151 MHz, Methanol-d_4) δ 170.4, 164.5, 141.7, 141.6, 138.9, 138.1, 129.7, 129.6, 129.3, 128.9, 128.5, 127.8, 127.5, 125.8, 115.5, 78.7, 35.4, 30.8, 29.3. UPLC-MS: m/z calculated $[M-H]^-$ for $C_{21}H_{19}O_3$, 319.13; found 318.9. Purity by anal. HPLC: 96% (254 nm).

(*E*)-2-(1-((*E*)-2,6-Dichlorostyryl)-5-hydroxy-5,7,8,9-tetrahydro-6H-benzo[7]annulen-6-ylidene)acetic acid (1m). The compound **1m** was prepared from **6m** (0.26 g, 0.67 mmol), $CeCl_3 \cdot 7H_2O$ (0.28 g, 0.74 mmol), $NaBH_4$ (0.10 g, 2.7 mmol) and MeOH (12 mL), using

general procedure A. Purification by preparative HPLC (gradient 40−79% B, eluent A (Milli-Q H_2O/TFA, 100:0.1) and eluent B (MeCN/Milli-Q H_2O/TFA, 90:10:0.1) at a flow rate of 20 mL·min^{-1}, over 12 min) yielded **1m** (51 mg, 20%) as a white solid. ^{1}H NMR (600 MHz, Methanol-d_4) δ 7.49 (d, J = 7.7 Hz, 2H), 7.45 – 7.41 (m, 3H), 7.26 (t, J = 7.7 Hz, 1H), 7.22 (t, J = 8.1 Hz, 1H), 6.84 (d, J = 16.4 Hz, 1H), 6.08 (s, 1H), 5.39 (s, 1H), 3.48 – 3.42 (m, 1H), 3.27 – 3.21 (m, 1H), 2.95 – 2.88 (m, 1H), 2.70 – 2.62 (m, 1H), 1.87 – 1.80 (m, 1H), 1.74 – 1.66 (m, 1H). ^{13}C NMR (151 MHz, Methanol-d_4) δ 170.5, 164.6, 143.0, 138.9, 137.4, 137.4, 136.1, 135.5, 129.8, 129.8, 127.8, 127.4, 127.4, 126.4, 115.4, 77.7, 30.6, 28.6, 28.0. UPLC-MS: m/z calculated [M-H]$^-$ for $C_{21}H_{17}Cl_2O_3$, 387.06; found 387.1. Purity by anal. HPLC: >99% (254 nm).

(*E*)-2-(5-Hydroxy-1-phenethyl-5,7,8,9-tetrahydro-6*H*-benzo[7]annulen-6-ylidene)acetic acid (1n). The compound **1n** was prepared from **6n** (0.13 g, 0.41 mmol)**,** $CeCl_3·7H_2O$ (0.17 g, 0.45 mmol), $NaBH_4$ (0.24 g, 6.1 mmol) and MeOH (5 mL), using general procedure A. Purification by preparative HPLC (gradient 30−100% B, eluent A (Milli-Q H_2O/TFA, 100:0.1) and eluent B (MeCN/Milli-Q H_2O/TFA, 90:10:0.1) at a flow rate of 20 mL·min^{-1}, over 12 min) yielded **1n** (58 mg, 26%) as a white solid. ^{1}H NMR (600 MHz, Methanol-d_4) δ 7.33 (d, J = 7.7 Hz, 1H), 7.25 – 7.21 (m, 2H), 7.16 – 7.12 (m, 3H), 7.09 (t, J = 7.6 Hz, 1H), 7.02 (dd, J = 7.6, 1.4 Hz, 1H), 6.04 (s, 1H), 5.34 (s, 1H), 3.44 – 3.39 (m, 1H), 3.19 – 3.13 (m, 1H), 2.95 – 2.91 (m, 2H), 2.85 – 2.77 (m, 3H), 2.71 – 2.65 (m, 1H), 1.82 – 1.74 (m, 1H), 1.69 – 1.62 (m, 1H). ^{13}C NMR (151 MHz, Methanol-d_4) δ 170.6, 164.7, 143.0, 142.8, 140.3, 138.8, 130.4, 129.5, 129.3, 127.3, 126.9, 125.5, 115.2, 78.1, 39.3, 37.1, 30.7, 28.6, 27.9. UPLC-MS: m/z calculated [M-H]$^-$ for $C_{21}H_{21}O_3$, 321.15, found 321.0. Purity by anal. HPLC: 98% (254 nm).

(*E*)-5-(2-Bromophenyl)pent-4-enoic acid (3a). The compound **3a** was prepared from **2a** (2.9 mL, 25.0 mmol), (3-carboxypropyl)-triphenylphosphoniumbromide (11.8 g, 27.5 mmol),

sodium bis(trimethylsilyl) amide solution (55.0 mL, 55.0 mmol) and THF (200 mL), using general procedure B. Purification by FC chromatography (Heptane/EtOAc 7:3 + 1% of AcOH) yielded **3a** and its (*Z*)-isomer with a ratio of 3:1 (6.1 g, 95%) as a white solid. ^{1}H NMR (400 MHz, Chloroform-*d*) δ 7.52 (dd, *J* = 8.0, 1.3 Hz, 1H), 7.47 (dd, *J* = 7.8, 1.7 Hz, 1H), 7.31 – 7.20 (m, 1H), 7.07 (td, *J* = 7.7, 1.7 Hz, 1H), 6.78 (d, *J* = 15.5 Hz, 1H), 6.25 – 6.11 (m, 1H), 2.66 – 2.53 (m, 4H). ^{13}C NMR (101 MHz, Chloroform-*d*) δ 178.1, 137.3, 133.0, 131.2, 130.3, 128.7, 127.6, 127.1, 123.4, 33.6, 28.1.

(*E*)-5-(3-Bromophenyl)pent-4-enoic acid (3b). The compound **3b** was prepared from **2b** (4.1 mL, 35.0 mmol), (3-carboxypropyl)-triphenylphosphoniumbromide (16.5 g, 38.5 mmol), sodium bis(trimethylsilyl) amide solution (77.0 mL, 77.0 mmol) and THF (220 mL), using general procedure B. Purification by FC chromatography (Heptane/EtOAc 7:3 + 1% of AcOH) yielded **3b** and its (*Z*)-isomer with a ratio of 5:1 (8.1 g, 91%) as a white solid. ^{1}H NMR (400 MHz, Chloroform-*d*) δ 7.49 (t, *J* = 1.8 Hz, 1H), 7.35 – 7.31 (m, 1H), 7.25 – 7.18 (m, 1H), 7.16 (t, *J* = 7.8 Hz, 1H), 6.38 (d, *J* = 15.9 Hz, 1H), 6.27 – 6.18 (m, 1H), 2.57 – 2.54 (m, 4H). ^{13}C NMR (101 MHz, Chloroform-*d*) δ 178.2, 139.6, 130.2, 130.2, 130.1, 129.8, 129.1, 124.9, 122.9, 33.6, 28.0.

(*E*)-5-(4-Bromophenyl)pent-4-enoic acid (3c). The compound **3c** was prepared from **2c** (2.5 g, 13.7 mmol), (3-carboxypropyl)-triphenylphosphoniumbromide (6.5 g, 15.0 mmol), sodium bis(trimethylsilyl) amide solution (30.0 mL, 30.0 mmol) and THF (130 mL), using general procedure B. Purification by FC chromatography (Heptane/EtOAc 7:3 + 1% of AcOH) yielded **3c** (3.0 g, 87%) as a white solid. ^{1}H NMR (400 MHz, Chloroform-*d*) δ 7.41 (d, *J* = 8.4 Hz, 2H), 7.20 (d, *J* = 8.5 Hz, 2H), 6.38 (d, *J* = 15.9 Hz, 1H), 6.27 – 6.14 (m, 1H), 2.56 – 2.51 (m, 4H). ^{13}C NMR (101 MHz, Chloroform-*d*) δ 179.0, 136.3, 131.7, 130.3, 129.0, 127.8, 121.1, 33.7, 28.0.

(*E*)-5-(3-Chlorophenyl)pent-4-enoic acid (3d). The compound **3d** was prepared from **2d** (1.8 mL, 16.0 mmol), (3-carboxypropyl)-triphenylphosphoniumbromide (7.6 g, 17.6 mmol), sodium bis(trimethylsilyl) amide solution (35.0 mL, 35.0 mmol) and THF (125 mL), using general procedure B. Purification by FC chromatography (Heptane/EtOAc 7:3 + 1% of AcOH) yielded **3d** (2.1 g, 63%) as a white solid. ^{1}H NMR (400 MHz, DMSO-*d*6) δ 7.45 – 7.43 (m, 1H), 7.34 – 7.32 (m, 2H), 7.27 – 7.24 (m, 1H), 6.45 – 6.35 (m, 2H), 2.42 – 2.39 (m, 4H). ^{13}C NMR (101 MHz, DMSO-*d*6) δ 174.2, 139.9, 133.9, 131.8, 130.8, 129.1, 127.2, 126.0, 125.0, 33.7, 28.3.

(*E*)-5-(*m*-Tolyl)pent-4-enoic acid (3e). The compound **3e** was prepared from **2e** (1.8 mL, 15.0 mmol), (3-carboxypropyl)-triphenylphosphoniumbromide (7.1 g, 16.5 mmol), sodium bis(trimethylsilyl) amide solution (33.0 mL, 33.0 mmol) and THF (110 mL), using general procedure B. Purification by FC chromatography (Heptane/EtOAc 7:3 + 1% of AcOH) yielded **3e** and its (*Z*)-isomer with a ratio of 7:1 (2.5 g, 89%) as a white solid. ^{1}H NMR (400 MHz, Chloroform-*d*) δ 7.24 – 7.12 (m, 3H), 7.03 (d, *J* = 7.3 Hz, 1H), 6.42 (d, *J* = 15.8 Hz, 1H), 6.25 – 6.15 (m, 1H), 2.58 – 2.52 (m, 4H), 2.34 (s, 3H). ^{13}C NMR (101 MHz, Chloroform-*d*) δ 178.3, 138.1, 137.2, 131.3, 128.4, 128.0, 127.8, 126.8, 123.3, 33.7, 27.9, 21.4.

(*E*)-5-([1,1'-Biphenyl]-3-yl)pent-4-enoic acid (3i). The compound **3i** was prepared from **2i** (2.5 mL, 15.0 mmol), (3-carboxypropyl)-triphenylphosphoniumbromide (7.1 g, 16.5 mmol), sodium bis(trimethylsilyl) amide solution (33.0 mL, 33.0 mmol) and THF (110 mL), using general procedure B. Purification by FC chromatography (Heptane/EtOAc 7:3 + 1% of AcOH) yielded **3i** and its (*Z*)-isomer with a ratio of 3.5:1 (3.5 g, 93%) as a white solid. ^{1}H NMR (400 MHz, Chloroform-*d*) δ 7.61 – 7.58 (m, 2H), 7.56 (t, *J* = 1.8 Hz, 1H), 7.49 – 7.31 (m, 6H), 6.52 (d, *J* = 15.6 Hz, 1H), 6.35 – 6.23 (m, 1H), 2.77 – 2.49 (m, 4H). ^{13}C NMR (101 MHz, Chloroform-*d*) δ 178.3, 141.7, 141.3, 137.9, 131.3, 129.1, 128.9, 128.6, 127.5, 127.3, 126.3, 125.2, 125.1, 33.7, 28.1.

5-(2-Bromophenyl)pentanoic acid (4a). The compound **4a** was prepared from **3a** and its (*Z*)-isomer (6.1 g, 23.8 mmol), Pd/C (1.1 g) and EtOAc (250 mL), using general procedure C. Compound **4a** (6.1 g, 100%) was afforded as orange oil and used directly for the next step without purification. f^{1}H NMR (400 MHz, Chloroform-*d*) δ 7.52 (d, *J* = 7.5 Hz, 1H), 7.24 – 7.15 (m, 2H), 7.05 (ddd, *J* = 8.0, 6.3, 2.7 Hz, 1H), 2.76 (t, *J* = 7.4 Hz, 2H), 2.42 (t, *J* = 7.1 Hz, 2H), 1.78 – 1.63 (m, 4H). ^{13}C NMR (151 MHz, Chloroform-*d*) δ 177.9, 141.4, 133.0, 130.4, 127.8, 127.6, 124.6, 35.9, 33.6, 29.4, 24.5.

5-(3-Bromophenyl)pentanoic acid (4b). The compound **4b** was prepared from **3b** and its (*Z*)-isomer (10.1 g, 39.6 mmol), Pd/C (0.81 g) and EtOAc (250 mL), using general procedure C. Compound **4b** (10.1 g, 99%) was afforded as brown oil and used directly for the next step without purification. ^{1}H NMR (600 MHz, Chloroform-*d*) δ 7.34 – 7.30 (m, 2H), 7.14 (t, *J* = 7.6 Hz, 1H), 7.09 (dt, *J* = 7.6, 1.4 Hz, 1H), 2.61 (t, *J* = 6.9 Hz, 2H), 2.41 – 2.35 (m, 2H), 1.71 – 1.64 (m, 4H). ^{13}C NMR (151 MHz, Chloroform-*d*) δ 178.9, 144.5, 131.6, 130.1, 129.1, 127.2, 122.6, 35.3, 33.8, 30.6, 24.3.

5-(4-Bromophenyl)pentanoic acid (4c). The compound **4c** was prepared from **3c** (2.3 g, 8.9 mmol), Pd/C (0.23 g) and EtOAc (100 mL), using general procedure C. Compound **4c** (1.6 g, 72%) was afforded as brown oil and used directly for the next step without purification. ^{1}H NMR (400 MHz, Chloroform-*d*) δ 7.39 (d, *J* = 8.3 Hz, 2H), 7.04 (d, *J* = 8.3 Hz, 2H), 2.59 (t, *J* = 6.9 Hz, 2H), 2.40 – 2.34 (m, 2H), 1.71 – 1.61 (m, 4H). ^{13}C NMR (101 MHz, Chloroform-*d*) δ 179.3, 141.0, 131.5, 130.3, 119.7, 35.1, 33.8, 30.7, 24.3.

5-(3-Chlorophenyl)pentanoic acid (4d). The compound **4d** was prepared from **3d** (2.1 g, 10.0 mmol), Pd/C (0.20 g) and EtOAc (100 mL), using general procedure C. Compound **4d** (2.0 g, 94%) was afforded as brown oil and used directly for the next step without purification. ^{1}H NMR (400 MHz, DMSO-*d*6) δ 7.30 (t, *J* = 7.7 Hz, 1H), 7.27 – 7.26 (m, 1H), 7.24 – 7.21 (m, 1H), 7.17 – 7.15 (m, 1H), 2.60 – 2.57 (m, 2H), 2.24 – 2.20 (m, 2H), 1.61 – 1.45 (m, 4H).

^{13}C NMR (101 MHz, DMSO-*d*6) δ 174.4, 144.7, 132.8, 130.0, 128.1, 127.0, 125.6, 34.3, 33.4, 30.1, 24.0.

5-(*m*-Tolyl)pentanoic acid (4e). The compound **4e** was prepared from **3e** its (*Z*)-isomer (2.5 g, 12.9 mmol), Pd/C (0.20 g) and EtOAc (100 mL), using general procedure C. Compound **4e** (2.4 g, 98%) was afforded as yellow oil and used directly for the next step without purification. ^{1}H NMR (400 MHz, Chloroform-*d*) δ 7.17 (t, *J* = 7.8 Hz, 1H), 7.03 – 6.95 (m, 3H), 2.63 – 2.57 (m, 2H), 2.43 – 2.36 (m, 2H), 2.33 (s, 3H), 1.76 – 1.60 (m, 4H). ^{13}C NMR (101 MHz, Chloroform-*d*) δ 179.4, 142.1, 138.0, 129.3, 128.4, 126.7, 125.5, 35.6, 33.9, 31.0, 24.5, 21.5.

5-([1,1'-Biphenyl]-3-yl)pentanoic acid (4i). The compound **4i** was prepared from **3i** its (*Z*)-isomer (13.3 g, 52.9 mmol), Pd/C (1.1 g) and EtOAc (500 mL), using general procedure C. Compound **4i** (13.4 g, 99%) was afforded as yellow oil and used directly for the next step without purification. ^{1}H NMR (400 MHz, Chloroform-*d*) δ 7.63 – 7.55 (m, 2H), 7.47 – 7.39 (m, 4H), 7.38 – 7.31 (m, 2H), 7.17 (dt, *J* = 7.5, 1.5 Hz, 1H), 2.76 – 2.67 (m, 2H), 2.44 – 2.37 (m, 2H), 1.78 – 1.69 (m, 4H). ^{13}C NMR (101 MHz, Chloroform-*d*) δ 179.4, 142.6, 141.5, 128.9, 128.8, 127.5, 127.4, 127.3, 127.3, 124.9, 35.8, 33.9, 30.9, 24.5.

1-Bromo-6,7,8,9-tetrahydro-5*H*-benzo[7]annulen-5-one (5a). The compound **5a** was prepared from **4a** (6.9 g, 26.7 mmol) and polyphosphoric acid (157.0 g, 1.6 mol), using general procedure D. Purification by FC chromatography (Heptane/EtOAc 9:1) yielded **5a** (2.3 g, 40%) as brown oil. ^{1}H NMR (400 MHz, Chloroform-*d*) δ 7.69 (dd, *J* = 7.9, 1.3 Hz, 1H), 7.53 (dd, *J* = 7.7, 1.3 Hz, 1H), 7.14 (t, *J* = 7.8 Hz, 1H), 3.10 (t, *J* = 6.2 Hz, 2H), 2.70 (t, *J* = 6.0 Hz, 2H), 1.91 – 1.82 (m, 2H), 1.82 – 1.73 (m, 2H). ^{13}C NMR (101 MHz, Chloroform-*d*) δ 206.3, 141.5, 139.4, 136.2, 128.1, 127.6, 124.9, 40.5, 31.0, 23.9, 20.8.

2-Bromo-6,7,8,9-tetrahydro-5*H*-benzo[7]annulen-5-one (5b). The compound **5b** was prepared from **4b** (10.3 g, 40.0 mmol) and polyphosphoric acid (52.8 g, 0.54 mol), using general procedure D. Purification by FC chromatography (Heptane/EtOAc 9:1) yielded **5b** (5.8

g, 60%) as brown oil. ^{1}H NMR (600 MHz, Chloroform-*d*) δ 7.59 (d, *J* = 8.2 Hz, 1H), 7.44 (dd, *J* = 8.3, 2.0 Hz, 1H), 7.38 (d, *J* = 1.9 Hz, 1H), 2.90 (t, *J* = 6.3 Hz, 2H), 2.72 (t, *J* = 6.1 Hz, 2H), 1.91 – 1.86 (m, 2H), 1.84 – 1.78 (m, 2H). ^{13}C NMR (151 MHz, Chloroform-*d*) δ 205.0, 143.3, 137.7, 132.7, 130.5, 130.1, 127.0, 40.9, 32.4, 25.2, 20.8.

3-Bromo-6,7,8,9-tetrahydro-5*H*-benzo[7]annulen-5-one (5c). The compound **5c** was prepared from **4c** (0.49 g, 1.9 mmol) and polyphosphoric acid (11.7 g, 0.12 mol), using general procedure D. Purification by FC chromatography (Heptane/EtOAc 9:1) yielded **5c** (0.24 g, 53%) as brown oil. ^{1}H NMR (600 MHz, Chloroform-*d*) δ 7.84 (d, *J* = 2.2 Hz, 1H), 7.52 (dd, *J* = 8.1, 2.3 Hz, 1H), 7.08 (d, *J* = 8.1 Hz, 1H), 2.88 (t, *J* = 6.0 Hz, 2H), 2.73 (t, *J* = 6.3 Hz, 2H), 1.90 – 1.84 (m, 2H), 1.84 – 1.79 (m, 2H). ^{13}C NMR (151 MHz, Chloroform-*d*) δ 204.6, 140.5, 140.2, 135.0, 131.6, 131.5, 120.7, 40.8, 32.1, 25.2, 20.9.

2-Chloro-6,7,8,9-tetrahydro-5*H*-benzo[7]annulen-5-one (5d). The compound **5d** was prepared from **4d** (1.9 g, 8.8 mmol) and polyphosphoric acid (10.8 g, 0.11 mol), using general procedure D. Purification by FC chromatography (Heptane/EtOAc 9:1) yielded **5d** (1.2 g, 73%) as brown oil. ^{1}H NMR (400 MHz, DMSO-*d*6) δ 7.60 (d, *J* = 8.3 Hz, 1H), 7.43 (d, *J* = 2.1 Hz, 1H), 7.40 (dd, *J* = 8.3, 2.1 Hz, 1H), 2.94 – 2.91 (m, 2H), 2.69 – 2.67 (m, 2H), 1.79 – 1.77 (m, 2H), 1.71 – 1.67 (m, 2H). ^{13}C NMR (101 MHz, DMSO-*d*6) δ 203.8, 143.7, 137.0, 136.7, 130.1, 129.4, 126.6, 40.1, 31.1, 24.5, 20.1.

2-Methyl-6,7,8,9-tetrahydro-5*H*-benzo[7]annulen-5-one (5e). The compound **5e** was prepared from **4e** (2.4 g, 12.6 mmol) and polyphosphoric acid (18.2 g, 0.19 mol), using general procedure D. Purification by FC chromatography (Heptane/EtOAc 9:1) yielded **5e** (2.1 g, 94%) as brown oil. ^{1}H NMR (400 MHz, Chloroform-*d*) δ 7.66 (d, *J* = 7.9 Hz, 1H), 7.11 (dd, *J* = 7.9, 1.7 Hz, 1H), 7.01 (d, *J* = 1.7 Hz, 1H), 2.89 (t, *J* = 6.0 Hz, 2H), 2.72 (t, *J* = 6.2 Hz, 2H), 2.36 (s, 3H), 1.93 – 1.74 (m, 4H). ^{13}C NMR (101 MHz, Chloroform-*d*) δ 205.7, 142.9, 141.7, 136.3, 130.6, 129.0, 127.5, 41.0, 32.7, 25.4, 21.6, 21.0.

2-Fluoro-6,7,8,9-tetrahydro-5*H*-benzo[7]annulen-5-one (5f). A mixture of **5b** (0.44 g, 1.9 mmol), bis(tributyltin) (2.2 g, 3.8 mmol) and $Pd(PPh_3)_4$ (0.23 g, 0.20 mmol) in anhydrous toluene (18 mL) was heated at reflux under argon atmosphere for 3 hours. After evaporation, quick purification by FC chromatography was performed and the resulting aromatic stannylene was re-dissolved in acetone (40 mL). Ag_2O (0.29 g, 1.2 mmol), $NaHCO_3$ (0.32 g, 3.7 mmol) and Selectfluor (1.0 g, 2.9 mmol) were added to the solution, which was then refluxed for 4 hours. The reaction mixture was filtered over a short pad of celite and evaporated *in vacuo* to dryness. Purification by FC chromatography (Heptane/EtOAc 9:1) yielded a mixture (0.18 g) of **5b**, **5f** and 6,7,8,9-tetrahydro-5*H*-benzo[7]annulen-5-one. For **5f**, ^{1}H NMR (400 MHz, Chloroform-*d*) δ 7.59 (d, *J* = 8.3 Hz, 1H), 7.44 (dd, *J* = 8.3, 2.0 Hz, 1H), 7.38 (d, *J* = 1.9 Hz, 1H), 2.90 (t, *J* = 7.2 Hz, 2H), 2.75 – 2.70 (m, 2H), 1.93 – 1.77 (m, 4H). ^{19}F NMR (376 MHz, Chloroform-*d*) δ -76.9.

2-Iodo-6,7,8,9-tetrahydro-5*H*-benzo[7]annulen-5-one (5g). A mixture of **5b** (0.27 g, 2.4 mmol), bis(tributyltin) (2.8 g, 4.8 mmol) and $Pd(PPh_3)_4$ (0.29 g, 0.24 mmol) in anhydrous toluene (22 mL) was heated at reflux under argon atmosphere for 3 hours. After evaporation, quick purification by FC chromatography was performed and the resulting aromatic stannylene was re-dissolved in THF (50 mL). I_2 (0.91 g, 3.6 mmol) in THF (35 mL) was added dropwise to the solution at 0 °C. After stirring for 1 hour at 0°C, the reaction was quenched by $NaBH_4$ and neutralized using saturated $NaHCO_3$ solution. The aqueous phase was extracted with EtOAc and the combined organic phases were dried over Na_2SO_4, filtered, and evaporated *in vacuo*. Purification by FC chromatography (Heptane/EtOAc 8:2) yielded **5g** (0.30 g, 44%) as brown oil. ^{1}H NMR (400 MHz, Chloroform-*d*) δ 7.66 (dd, *J* = 8.2, 1.7 Hz, 1H), 7.61 (d, *J* = 1.7 Hz, 1H), 7.43 (d, *J* = 8.1 Hz, 1H), 2.87 (t, *J* = 7.2 Hz, 2H), 2.75 – 2.68 (m, 2H), 1.93 – 1.75 (m, 4H). ^{13}C NMR (101 MHz, Chloroform-*d*) δ 205.3, 143.2, 138.7, 138.3, 136.1, 130.3, 99.9, 40.9, 32.3, 25.2, 20.9.

1-Phenyl-6,7,8,9-tetrahydro-5*H*-benzo[7]annulen-5-one (5h). The compound **5h** was prepared from **5a** (0.25 g, 1.0 mmol), phenylboronic acid (0.26 g, 2.1 mmol), $Pd(PPh_3)_4$ (0.11 g, 0.10 mmol), K_2CO_3 (0.44 g, 3.1 mmol), DMF (24 mL) and H_2O (16 mL), using general procedure E. Purification by FC chromatography (Heptane/EtOAc 9:1) yielded **5h** (0.22 g, 90%) as yellow oil. ^{1}H NMR (400 MHz, Chloroform-*d*) δ 7.64 (dd, *J* = 7.5, 1.6 Hz, 1H), 7.48 – 7.27 (m, 6H), 7.25 – 7.18 (m, 1H), 2.79 – 2.70 (m, 4H), 1.89 – 1.75 (m, 4H). ^{13}C NMR (101 MHz, Chloroform-*d*) δ 207.8, 141.3, 140.5, 137.7, 133.8, 129.8, 129.4, 128.3, 127.8, 127.4, 126.4, 40.9, 28.1, 25.8, 21.0.

2-Phenyl-6,7,8,9-tetrahydro-5*H*-benzo[7]annulen-5-one (5i). The compound **5i** was prepared by using two different methods.

Method 1: **5i** was synthesized from **5b** (0.10 g, 0.42 mmol), phenylboronic acid (0.10 g, 0.83 mmol), $Pd(PPh_3)_4$ (96 mg, 0.08 mmol), K_2CO_3 (0.17 g, 1.2 mmol), DMF (16 mL) and H_2O (8 mL), using general procedure E. Purification by FC chromatography (Heptane/EtOAc 9:1) yielded **5i** (65 mg, 69%) as yellow oil. ^{1}H NMR (600 MHz, Chloroform-*d*) δ 7.83 (d, *J* = 8.0 Hz, 1H), 7.64 – 7.58 (m, 2H), 7.53 (dd, *J* = 8.0, 1.8 Hz, 1H), 7.50 – 7.42 (m, 3H), 7.39 (tt, *J* = 7.4, 1.3 Hz, 1H), 3.01 (t, *J* = 6.2 Hz, 2H), 2.77 (t, *J* = 6.1 Hz, 2H), 1.97 – 1.90 (m, 2H), 1.90 – 1.81 (m, 2H). ^{13}C NMR (151 MHz, Chloroform-*d*) δ 205.7, 145.1, 142.1, 140.2, 137.7, 129.5, 129.0, 128.6, 128.1, 127.4, 125.5, 41.1, 32.9, 25.4, 21.0.

Method 2: **5i** was also prepared from **4i** (16.4 g, 0.06 mol) and polyphosphoric acid (82.5 g, 0.81 mol), using general procedure D. Purification by FC chromatography (Heptane/EtOAc 9:1) yielded **5i** (7.8 g, 51%) as yellow oil.

3-Phenyl-6,7,8,9-tetrahydro-5*H*-benzo[7]annulen-5-one (5j). The compound **5j** was prepared from **5c** (0.32 g, 1.3 mmol), phenylboronic acid (0.33 g, 2.7 mmol), $Pd(PPh_3)_4$ (0.16 g, 0.14 mmol), K_2CO_3 (0.56 g, 4.0 mmol), DMF (24 mL) and H_2O (16 mL), using general procedure E. Purification by FC chromatography (Heptane/EtOAc 9:1) yielded **5j** (0.23 g,

73%) as yellow oil. ^{1}H NMR (400 MHz, Chloroform-*d*) δ 7.98 (d, *J* = 2.1 Hz, 1H), 7.66 (dd, *J* = 7.8, 2.1 Hz, 1H), 7.65 – 7.57 (m, 2H), 7.48 – 7.38 (m, 2H), 7.34 (tt, *J* = 7.4, 1.3 Hz, 1H), 7.28 (d, *J* = 7.8 Hz, 1H), 2.98 (t, *J* = 5.6 Hz, 2H), 2.77 (t, *J* = 6.3 Hz, 2H), 1.98 – 1.78 (m, 4H). ^{13}C NMR (101 MHz, Chloroform-*d*) δ 206.2, 140.5, 140.2, 139.8, 139.3, 130.7, 130.5, 129.0, 127.6, 127.3, 127.1, 41.1, 32.4, 25.4, 21.2.

(*E*)-1-Styryl-6,7,8,9-tetrahydro-5*H*-benzo[7]annulen-5-one (5k). The compound **5k** was prepared from **5a** (0.24 g, 1.0 mmol), styrene (0.23 mL, 2.0 mmol), $Pd(OAc)_2$ (33 mg, 0.15 mmol), PPh_3 (80 mg, 0.30 mmol), K_2CO_3 (0.27 g, 2.0 mmol) and anhydrous DMF (8 mL), using general procedure F. Purification by FC chromatography (Heptane/EtOAc 8:2) yielded **5k** (0.14 g, 54%) as brown oil. ^{1}H NMR (600 MHz, Chloroform-*d*) δ 7.70 (dd, *J* = 7.7, 1.4 Hz, 1H), 7.55 – 7.51 (m, 3H), 7.43 – 7.36 (m, 3H), 7.32 – 7.28 (m, 2H), 6.96 (d, *J* = 16.0 Hz, 1H), 3.01 (t, *J* = 6.5 Hz, 2H), 2.70 (t, *J* = 6.0 Hz, 2H), 1.89 (p, *J* = 6.7 Hz, 2H), 1.83 – 1.77 (m, 2H). ^{13}C NMR (151 MHz, Chloroform-*d*) δ 207.8, 140.6, 137.8, 137.4, 136.7, 132.4, 130.1, 128.9, 128.1, 127.7, 126.9, 126.8, 126.0, 40.7, 27.2, 24.7, 20.8.

(*E*)-2-Styryl-6,7,8,9-tetrahydro-5*H*-benzo[7]annulen-5-one (5l). The compound **5l** was prepared from **5b** (0.42 g, 1.7 mmol), styrene (0.40 mL, 3.4 mmol), $Pd(OAc)_2$ (58 mg, 0.26 mmol), PPh_3 (0.15 g, 0.52 mmol), K_2CO_3 (0.48 g, 3.4 mmol) and anhydrous DMF (14 mL), using general procedure F. Purification by FC chromatography (Heptane/EtOAc 9:1) yielded **5l** (0.18 g, 40%) as orange oil. ^{1}H NMR (400 MHz, Chloroform-*d*) δ 7.76 (d, *J* = 8.0 Hz, 1H), 7.55 – 7.51 (m, 2H), 7.45 (dd, *J* = 8.1, 1.8 Hz, 1H), 7.41 – 7.32 (m, 3H), 7.29 (tt, *J* = 7.2, 1.3 Hz, 1H), 7.21 (d, *J* = 16.3 Hz, 1H), 7.10 (d, *J* = 16.3 Hz, 1H), 2.97 (t, *J* = 6.1 Hz, 2H), 2.75 (t, *J* = 6.1 Hz, 2H), 1.98 – 1.78 (m, 4H). ^{13}C NMR (101 MHz, Chloroform-*d*) δ 205.4, 142.1, 141.3, 137.8, 137.0, 131.0, 129.5, 128.9, 128.3, 128.0, 127.8, 126.9, 124.7, 41.0, 32.8, 25.3, 21.0.

(*E*)-1-(2,6-Dichlorostyryl)-6,7,8,9-tetrahydro-5*H*-benzo[7]annulen-5-one (5m). The compound **5m** was prepared from **5a** (0.24 g, 1.0 mmol), 2,6-dichlorostyrene (0.28 mL, 2.0 mmol), $Pd(OAc)_2$ (24 mg, 0.10 mmol), PPh_3 (55 mg, 0.20 mmol), K_2CO_3 (0.28 g, 2.0 mmol) and anhydrous DMF (8 mL), using general procedure F. Purification by FC chromatography (Heptane/EtOAc 9:1) yielded **5m** (0.19 g, 59%) as a yellow solid. ^{1}H NMR (400 MHz, Chloroform-*d*) δ 7.75 (dd, *J* = 7.8, 1.4 Hz, 1H), 7.58 (dd, *J* = 7.6, 1.4 Hz, 1H), 7.44 (d, *J* = 16.6 Hz, 1H), 7.40 – 7.31 (m, 3H), 7.14 (t, *J* = 8.1 Hz, 1H), 6.94 (d, *J* = 16.5 Hz, 1H), 3.00 (t, *J* = 6.3 Hz, 2H), 2.74 – 2.67 (m, 2H), 1.92 – 1.75 (m, 4H). ^{13}C NMR (101 MHz, Chloroform-*d*) δ 207.6, 140.5, 138.2, 136.4, 134.9, 134.7, 132.3, 130.4, 128.8, 128.5, 128.2, 127.0, 126.1, 40.7, 27.3, 24.7, 20.7.

1-Phenethyl-6,7,8,9-tetrahydro-5*H*-benzo[7]annulen-5-one (5n). The compound **5n** was prepared from **5k** (0.18 g, 0.69 mmol), Pd/C (51 mg) and EtOAc (8 mL), using general procedure C. Compound **5n** (0.18 g, 97%) was afforded as yellow oil and used directly for the next step without purification.

(*E*)-2-(1-Bromo-5-oxo-5,7,8,9-tetrahydro-6*H*-benzo[7]annulen-6-ylidene)acetic acid (6a). The compound **6a** was prepared from **5a** (0.19 g, 0.80 mmol), glyoxylic acid monohydrate (0.30 g, 3.2 mmol), NaOH (0.19 g, 4.8 mmol), EtOH (7 mL) and H_2O (10 mL), using general procedure G. Purification by FC chromatography (CH_2Cl_2/MeOH 95:5 + 1% AcOH) yielded **6a** (0.17 g, 73%) as a yellow solid. ^{1}H NMR (600 MHz, Methanol-d_4) δ 7.82 (dd, *J* = 8.0, 1.3 Hz, 1H), 7.65 (dd, *J* = 7.6, 1.3 Hz, 1H), 7.27 (t, *J* = 8.0 Hz, 1H), 6.77 (s, 1H), 3.06 (t, *J* = 6.8 Hz, 2H), 2.78 (t, *J* = 6.7 Hz, 2H), 2.01 – 1.98 (m, 2H). ^{13}C NMR (151 MHz, Methanol-d_4) δ 197.4, 169.0, 151.9, 140.5, 140.0, 138.2, 131.6, 129.6, 126.8, 125.3, 31.0, 26.0, 24.9.

(*E*)-2-(2-Bromo-5-oxo-5,7,8,9-tetrahydro-6*H*-benzo[7]annulen-6-ylidene)acetic acid (6b). The compound **6b** was prepared from **5b** (4.5 g, 18.9 mmol), glyoxylic acid monohydrate (6.9 g, 75.5 mmol), NaOH (4.7 g, 0.12 mol), EtOH (40 mL) and H_2O (120 mL), using general

procedure G. Purification by FC chromatography (CH_2Cl_2/MeOH 95:5 + 1% AcOH) yielded **6b** (4.0 g, 73%) as a yellow solid. ^{1}H NMR (400 MHz, Methanol-d_4) δ 7.65 (d, J = 8.3 Hz, 1H), 7.55 (dd, J = 8.3, 2.0 Hz, 1H), 7.50 (d, J = 2.0 Hz, 1H), 6.68 (s, 1H), 2.84 – 2.77 (m, 4H), 2.05 (q, J = 6.8 Hz, 2H). ^{13}C NMR (101 MHz, Methanol-d_4) δ 197.5, 169.0, 153.1, 143.9, 137.0, 133.5, 132.0, 131.4, 128.9, 126.4, 32.0, 26.1, 26.0.

(*E*)-2-(3-Bromo-5-oxo-5,7,8,9-tetrahydro-6*H*-benzo[7]annulen-6-ylidene)acetic acid (6c). The compound **6c** was prepared from **5c** (0.24 g, 1.0 mmol), glyoxylic acid monohydrate (0.37 g, 4.0 mmol), NaOH (0.25 g, 6.0 mmol), EtOH (7 mL) and H_2O (10 mL), using general procedure G. Purification by FC chromatography (CH_2Cl_2/MeOH 95:5 + 1% AcOH) yielded **6c** (0.26 g, 83%) as a yellow solid. ^{1}H NMR (400 MHz, Methanol-d_4) δ 7.83 (d, J = 2.2 Hz, 1H), 7.67 (dd, J = 8.1, 2.2 Hz, 1H), 7.22 (d, J = 8.1 Hz, 1H), 6.69 (s, 1H), 2.80 (t, J = 6.8 Hz, 4H), 2.03 (p, J = 6.9 Hz, 2H). ^{13}C NMR (101 MHz, Methanol-d_4) δ 197.0, 169.0, 152.7, 140.8, 139.8, 137.1, 132.8, 132.7, 126.7, 121.6, 31.7, 26.1, 26.0.

(*E*)-2-(2-Chloro-5-oxo-5,7,8,9-tetrahydro-6*H*-benzo[7]annulen-6-ylidene)acetic acid (6d). The compound **6d** was prepared from **5d** (1.2 g, 6.2 mmol), glyoxylic acid monohydrate (2.3 g, 24.7 mmol), NaOH (1.5 g, 37.1 mmol), EtOH (40 mL) and H_2O (40 mL), using general procedure G. Purification by FC chromatography (CH_2Cl_2/MeOH 95:5 + 1% AcOH) yielded **6d** (0.76 g, 49%) as a yellow solid. ^{1}H NMR (400 MHz, DMSO-*d*6) δ 7.70 – 7.68 (m, 1H), 7.49 – 7.47 (m, 2H), 6.56 (s, 1H), 2.80 – 2.76 (m, 2H), 2.70 – 2.67 (m, 2H), 1.97 – 1.92 (m, 2H) ^{1}H NMR (400 MHz, DMSO-*d*6) δ 195.4, 166.8, 150.6, 142.4, 137.8, 135.2, 130.9, 129.3, 127.1, 125.6, 30.2, 24.7, 24.4.

(*E*)-2-(2-Methyl-5-oxo-5,7,8,9-tetrahydro-6*H*-benzo[7]annulen-6-ylidene)acetic acid (6e). The compound **6e** was prepared from **5e** (4.8 g, 27.8 mmol), glyoxylic acid monohydrate (10.3 g, 0.11 mol), NaOH (6.7 g, 0.17 mol), EtOH (40 mL) and H_2O (40 mL), using general procedure G. Purification by FC chromatography (CH_2Cl_2/MeOH 95:5 + 1% AcOH) yielded

6e (5.4 g, 85%) as a yellow solid. ^{1}H NMR (600 MHz, Methanol-d_4) δ 7.66 (d, J = 7.8 Hz, 1H), 7.20 (dd, J = 7.9, 1.7 Hz, 1H), 7.10 (d, J = 1.7 Hz, 1H), 6.64 (s, 1H), 2.79 (td, J = 6.9, 2.1 Hz, 4H), 2.39 (s, 3H), 2.02 (p, J = 6.9 Hz, 2H). ^{13}C NMR (150MHz, Methanol-d_4) δ 198.6, 169.1, 154.2, 145.7, 142.1, 135.3, 131.3, 130.5, 128.9, 125.7, 32.4, 26.4, 26.1, 21.5.

(*E*)-2-(2-Fluoro-5-oxo-5,7,8,9-tetrahydro-6*H*-benzo[7]annulen-6-ylidene)acetic acid (6f). The compound **6f** was prepared from a mixture (0.18 g) of **5b**, **5f** and 6,7,8,9-tetrahydro-5*H*-benzo[7]annulen-5-one, glyoxylic acid monohydrate (0.37 g, 4.0 mol), NaOH (0.22 g, 5.6 mol), EtOH (16 mL) and H_2O (8 mL), using general procedure G. Purification by FC chromatography (CH_2Cl_2/MeOH 95:5 + 1% AcOH) yielded a mixture (0.14 g) of **6b**, **6f** and (*E*)-2-(5-oxo-5,7,8,9-tetrahydro-6*H*-benzo[7]annulen-6-ylidene)acetic acid. For **6f**, ^{1}H NMR (400 MHz, Methanol-d_4) δ 7.64 (d, J = 8.3 Hz, 1H), 7.57 – 7.53 (m, 1H), 7.50 (d, J = 1.9 Hz, 1H), 6.68 (s, 1H), 2.87 – 2.76 (m, 4H), 2.08 – 2.00 (m, 2H). ^{19}F NMR (376 MHz, Methanol-d_4) δ -108.1. UPLC-MS: m/z calculated $[M-H]^-$ for $C_{13}H_{10}FO_3$ = 233.06, found 233.0.

(*E*)-2-(2-Iodo-5-oxo-5,7,8,9-tetrahydro-6*H*-benzo[7]annulen-6-ylidene)acetic acid (6g). The compound **6g** was prepared from **5g** (0.27 g, 1.0 mmol), glyoxylic acid monohydrate (0.35 g, 3.8 mmol), NaOH (0.22 g, 5.3 mmol), EtOH (6 mL) and H_2O (10 mL), using general procedure G. Purification by FC chromatography (CH_2Cl_2/MeOH 95:5 + 1% AcOH) yielded **6g** (0.15 g, 46%) as a brown solid. ^{1}H NMR (400 MHz, Methanol-d_4) δ 7.77 (dd, J = 8.1, 1.7 Hz, 1H), 7.72 (d, J = 1.7 Hz, 1H), 7.47 (d, J = 8.1 Hz, 1H), 6.68 (s, 1H), 2.82 – 2.76 (m, 4H), 2.07 – 1.98 (m, 2H). ^{13}C NMR (101 MHz, Methanol-d_4) δ 198.2, 169.3, 153.3, 143.7, 139.6, 137.6, 137.5, 131.7, 126.5, 102.0, 31.8, 26.2, 24.2.

(*E*)-2-(5-Oxo-1-phenyl-5,7,8,9-tetrahydro-6*H*-benzo[7]annulen-6-ylidene)acetic acid (6h). The compound **6h** was prepared from **5h** (0.21 g, 0.90 mmol), glyoxylic acid monohydrate (0.33 g, 3.6 mmol), NaOH (0.21 g, 5.3 mmol), EtOH (8 mL) and H_2O (8 mL), using general procedure G. Purification by FC chromatography (CH_2Cl_2/MeOH 95:5 + 1%

AcOH) yielded **6h** (0.19 g, 72%) as a yellow solid. ^{1}H NMR (600 MHz, Methanol-d_4) δ 7.72 (dd, J = 7.6, 1.5 Hz, 1H), 7.48 – 7.38 (m, 5H), 7.32 – 7.29 (m, 2H), 6.75 (s, 1H), 2.89 (t, J = 6.7 Hz, 2H), 2.68 (t, J = 6.9 Hz, 2H), 1.94 (p, J = 6.8 Hz, 2H). ^{13}C NMR (151 MHz, Methanol-d_4) δ 198.9, 169.1, 152.9, 143.9, 142.2, 139.4, 138.3, 135.7, 130.3, 129.6, 129.4, 128.5, 127.7, 126.0, 28.0, 26.7, 26.3.

(*E*)-2-(5-Oxo-2-phenyl-5,7,8,9-tetrahydro-6*H*-benzo[7]annulen-6-ylidene)acetic acid (6i). The compound **6i** was prepared from **5i** (5.8 g, 24.7 mmol), glyoxylic acid monohydrate (9.1 g, 98.7 mmol), NaOH (6.1 g, 0.15 mol), EtOH (50 mL) and H_2O (150 mL), using general procedure G. Purification by FC chromatography (CH_2Cl_2/MeOH 95:5 + 1% AcOH) yielded **6i** (3.4 g, 47%) as a yellow solid. ^{1}H NMR (600 MHz, DMSO-d_6) δ 7.79 – 7.74 (m, 3H), 7.71 (dd, J = 8.0, 1.9 Hz, 1H), 7.65 (d, J = 1.8 Hz, 1H), 7.52 – 7.48 (m, 2H), 7.43 (tt, J = 7.3, 1.3 Hz, 1H), 6.57 (s, 1H), 2.86 (t, J = 6.9 Hz, 2H), 2.73 (t, J = 6.8 Hz, 2H), 1.98 (p, J = 6.9 Hz, 2H). ^{13}C NMR (151 MHz, DMSO-d_6) δ 196.1, 167.0, 151.4, 144.8, 140.9, 138.9, 135.2, 129.8, 129.1, 128.4, 127.9, 127.0, 125.2, 125.2, 30.8, 24.9, 24.6.

(*E*)-2-(5-Oxo-3-phenyl-5,7,8,9-tetrahydro-6*H*-benzo[7]annulen-6-ylidene)acetic acid (6j). The compound **6j** was prepared from **5j** (0.23 g, 1.0 mmol), glyoxylic acid monohydrate (0.38 g, 3.9 mmol), NaOH (0.24 g, 5.9 mmol), EtOH (10 mL) and H_2O (5 mL), using general procedure G. Purification by FC chromatography (CH_2Cl_2/MeOH 95:5 + 1% AcOH) yielded **6j** (84 mg, 29%) as a white solid. ^{1}H NMR (400 MHz, Methanol-d_4) δ 7.98 (d, J = 2.1 Hz, 1H), 7.80 (dd, J = 7.8, 2.1 Hz, 1H), 7.66 – 7.62 (m, 2H), 7.48 – 7.43 (m, 2H), 7.39 – 7.33 (m, 2H), 6.72 (s, 1H), 2.89 – 2.82 (m, 4H), 2.09 – 2.04 (m, 2H). ^{13}C NMR (101 MHz, Methanol-d_4) δ 197.2, 167.7, 152.2, 139.8, 139.4, 137.0, 133.2, 131.4, 130.0, 128.6, 127.3, 127.1, 126.4, 124.7, 30.5, 25.0, 24.8.

(*E*)-2-(5-Oxo-1-((*E*)-styryl)-5,7,8,9-tetrahydro-6*H*-benzo[7]annulen-6-ylidene)acetic acid (6k). The compound **6k** was prepared from **5k** (0.12 g, 0.45 mmol), glyoxylic acid

monohydrate (0.17 g, 1.8 mmol), NaOH (0.11 g, 2.7 mmol), EtOH (6 mL) and H_2O (3 mL), using general procedure G. Purification by FC chromatography (CH_2Cl_2/MeOH 95:5 + 1% AcOH) yielded **6k** (87 mg, 61%) as a yellow solid. ^{1}H NMR (600 MHz, Methanol-d_4) δ 7.85 (dd, J = 7.8, 1.3 Hz, 1H), 7.61 – 7.56 (m, 3H), 7.51 (d, J = 16.1 Hz, 1H), 7.40 – 7.34 (m, 3H), 7.27 (tt, J = 7.4, 1.3 Hz, 1H), 7.06 (d, J = 16.1 Hz, 1H), 6.77 (s, 1H), 2.97 (t, J = 6.8 Hz, 2H), 2.82 (t, J = 6.7 Hz, 2H), 2.04 (p, J = 6.7 Hz, 2H). ^{13}C NMR (151 MHz, Methanol-d_4) δ 198.9, 169.1, 152.8, 139.5, 138.7, 138.6, 138.0, 133.9, 132.1, 129.8, 129.4, 129.0, 128.2, 127.8, 126.2, 126.1, 27.2, 26.2, 25.8.

(*E*)-2-(5-Oxo-2-((*E*)-styryl)-5,7,8,9-tetrahydro-6*H*-benzo[7]annulen-6-ylidene)acetic acid (6l). The compound **6l** was prepared from **5l** (0.17 g, 0.64 mmol), glyoxylic acid monohydrate (0.24 g, 2.5 mmol), NaOH (0.16 g, 4.0 mmol), EtOH (10 mL) and H_2O (5 mL), using general procedure G. Purification by FC chromatography (CH_2Cl_2/MeOH 95:5 + 1% AcOH) yielded **6l** (0.13 g, 63%) as a yellow solid. ^{1}H NMR (400 MHz, Methanol-d_4) δ 7.77 (d, J = 8.0 Hz, 1H), 7.62 – 7.57 (m, 3H), 7.47 (d, J = 1.8 Hz, 1H), 7.39 – 7.33 (m, 3H), 7.28 (tt, J = 7.4, 1.3 Hz, 1H), 7.22 (d, J = 16.4 Hz, 1H), 6.67 (s, 1H), 2.89 – 2.80 (m, 4H), 2.06 (p, J = 6.9 Hz, 2H). ^{13}C NMR (101 MHz, Methanol-d_4) δ 198.2, 169.1, 154.2, 144.2, 142.6, 138.4, 136.8, 132.7, 130.9, 129.8, 129.3, 128.7, 128.5, 127.9, 126.0, 125.8, 32.5, 26.4, 26.1.

(*E*)-2-(1-((*E*)-2,6-Dichlorostyryl)-5-oxo-5,7,8,9-tetrahydro-6*H*-benzo[7]annulen-6-ylidene) acetic acid (6m). The compound **6m** was prepared from **5m** (0.17 g, 0.50 mmol), glyoxylic acid monohydrate (0.19 g, 2.0 mmol), NaOH (0.13 g, 3.2 mmol), EtOH (5 mL) and H_2O (5 mL), using general procedure G. Purification by FC chromatography (CH_2Cl_2/MeOH 95:5 + 1% AcOH) yielded **6m** (0.15 g, 77%) as a yellow solid. ^{1}H NMR (600 MHz, Methanol-d_4) δ 7.87 (dd, J = 7.8, 1.4 Hz, 1H), 7.67 (dd, J = 7.6, 1.4 Hz, 1H), 7.49 – 7.42 (m, 4H), 7.25 (t, J = 8.1 Hz, 1H), 7.00 (d, J = 16.4 Hz, 1H), 6.78 (s, 1H), 2.96 (t, J = 6.8 Hz, 2H), 2.82 (t, J = 6.7 Hz, 2H), 2.05 – 1.99 (m, 2H). ^{13}C NMR (151 MHz, Methanol-d_4) δ 198.7, 169.2, 152.4,

139.6, 138.9, 137.5, 135.8, 135.6, 135.6, 132.3, 130.1, 129.9, 129.9, 128.4, 127.6, 126.4, 27.4, 26.2, 25.9.

(*E*)-2-(5-Oxo-1-phenethyl-5,7,8,9-tetrahydro-6*H*-benzo[7]annulen-6-ylidene)acetic acid (6n). The compound **6n** was prepared from **5n** (0.18 g, 0.65 mmol), glyoxylic acid monohydrate (0.24 g, 2.6 mmol), NaOH (0.16 g, 3.9 mmol), EtOH (7 mL) and H_2O (7 mL), using general procedure G. Purification by FC chromatography (CH_2Cl_2/MeOH 95:5 + 1% AcOH) yielded **6n** (0.13 g, 59%) as a yellow solid. ^{1}H NMR (600 MHz, Methanol-d_4) δ 7.50 (dd, J = 7.6, 1.4 Hz, 1H), 7.38 (dd, J = 7.6, 1.4 Hz, 1H), 7.25 – 7.21 (m, 3H), 7.18 – 7.11 (m, 3H), 6.75 (s, 1H), 3.02 (t, J = 7.4 Hz, 2H), 2.89 (t, J = 7.3 Hz, 2H), 2.80 (t, J = 6.8 Hz, 2H), 2.73 (t, J = 6.7 Hz, 2H), 1.87 (p, J = 6.8 Hz, 2H). ^{13}C NMR (151 MHz, Methanol-d_4) δ 199.4, 175.2, 152.2, 142.6, 140.8, 139.6, 138.9, 135.8, 129.6, 129.4, 128.3, 127.8, 127.1, 126.3, 39.1, 36.0, 26.7, 26.3, 26.1.

Radioligand Binding Assays. *Compounds and Radioligands.* [^{3}H]NCS-382 (20 Ci/mmol, #ART-1114) was purchased from Biotrend (Köln, Germany) and [^{3}H]HOCPCA[35] (28.6 Ci/mmol) was prepared as described previously.

Cell Culturing and Transfection of HEK293T Cells. The HEK293T cells (#CRL-3216, ATTC) were maintained at 37 °C and 5% CO_2 in DMEM GlutaMax (#61965026, Gibco) supplemented with 10% fetal bovine serum (#10270106, Gibco) and 1% penicillin-streptomycin (#15140122, Invitrogen). For transfection, 4.5 mio cells were seeded in a 15-cm culture dish and transfected with the CaMKIIα construct the following day using 16 µg of plasmid DNA and 48 µL of PEI (Polysciences Inc.) diluted in 2 mL of a serum-free medium. Two days post-transfection, the cells were harvested in ice-cold PBS by scraping followed by centrifugation for 5 min at 1,500 x g. The resulting pellet was resuspended in ice-cold binding buffer (50 mM KH_2PO_4, pH 6) and homogenized using 2x zirconium beads using a Bullet

Blender (NextAdvance) at max speed for 20 sec. The protein concentration of the resulting whole cell homogenate was determined using Bradford according to the manufacturer's protocol, and homogenates were stored at -20 °C until further use.

[^{3}H]HOCPCA and [^{3}H]NCS-382 Competition Binding Assays. The well-established radioligand binding assay was performed using rat cortical membrane homogenates (native CaMKII) derived from adult male rats purchased from Janvier (RRID: RGD_7246927, France), as previously described[5, 31, 35] or whole cell lysates of transfected HEK293-T cells (recombinant rat CaMKIIα) in all cases using a 50 mM KH_2PO_4 buffer (pH 6.0). Protein samples were prepared exactly as previously described.[5] For the native binding assays, membrane homogenate with a final protein concentration of approximately 25 µg per well, was incubated with 16 nM [^{3}H]NCS-382 or 10 nM [^{3}H]HOCPCA together with increasing concentrations of NCS-382 for 1 h on ice. 1 mM GHB was used to determine non-specific binding (NSB). The reaction was terminated by rapid filtration through GF/C filter plates (PerkinElmer), and three rapid washes with ice-cold buffer using a 96-well harvester (Packard). The filter plates were dried, 30 µL of MicroScint-0 was added and the counts per minute (CPM) values determined in a TopCount NXT Microplate Scintillation counter (PerkinElmer). For the recombinant binding assay, 100-200 µg protein (whole cell lysates) per well was incubated with 40 nM [^{3}H]HOCPCA on ice using 10 mM GHB for NSB (total volume of 400 µL). After incubation for 1 h to reach equilibrium, soluble proteins were precipitated with ice-cold acetone and the reaction terminated by rapid filtration through GF/C unifilters (Whatman Schleicher and Schuell, Keene, NH), and three rapid washes with ice-cold buffer using a 48-well harvester (Alpha Biotech). Individual filters were dried, 3 mL of Opti-Fluor (PerkinElmer) was added and CPM values determined in a Packard Tricarb 2100 liquid scintillation counter.

Data Analysis. For binding experiments, specific binding was corrected for NSB and normalized to the total binding. Competition inhibition curves were analyzed using the 'One

site-Fit logIC_{50}' model in GraphPad Prism v. 9, and the K_I values were acquired *via* th Cheng-Prusoff equation:

$$K_I = \frac{IC_{50}}{1 + [RL]/K_D}$$

where [RL] denotes the specific radioligand concentration from each experiment and K_D is the dissociation constant of the radioligand ([^{3}H]HOCPCA, native = 259 nM, [^{3}H]NCS-382 = 430 nM), and [^{3}H]HOCPCA, recombinant =1.8 μM).[5] Data are summarized as mean ± S.E.M. from three to four independent experiments performed in triplicates.

Biophysical Assays. *Hub Protein Expression and Purification*. For the biophysical test panel purified human CaMKIIα hub domain proteins (either WT of 6x hub) were used (UniprotKB Q9UQM7, residues 345-475). The 6x hub construct contains six mutations (Thr354Asn, Glu355Gln, Thr412Asn, Ile414Met, Ile464His, and Phe467Met). Proteins were expressed and purified as previously described.[5, 6, 29, 30] Fraction purity was assessed by SDS-PAGE.

Surface Plasmon Resonance (SPR). SPR binding studies were performed at 25°C using a Pioneer FE instrument (Molecular Devices, FortéBio). Recombinant CaMKIIα hub 6x mutation protein was immobilized by amine coupling on to a biosensor surface to 6183 RU, using a 20 mM NaAc pH 5 immobilization buffer. Compounds in 2-fold dilution series was injected in order of increasing concentration over the immobilized CaMKIIα hub. An HBS-P (10 mM N-2-hydroxyethylpiperazine-N'-2-ethane sulfonic acid (HEPES), 150 mM NaCl, 0.005% Tween, 1 mM DTT) pH 6 running buffer was used. The data were analyzed using Qdat Data Analysis Tool version 2.6.3.0 (Molecular Devices, FortéBio). The sensorgrams were corrected for buffer bulk effects and unspecific binding of the samples to the chip matrix by blank and reference surface subtraction (activated flow cell channel by injection of EDC/NHS and inactivated by injection of ethanolamine). The equilibrium dissociation constants (K_D) were estimated by plotting responses at equilibrium (*R*eq) against the injected concentration

and curve fitted to a Langmuir (1:1) binding isotherm. Kinetic rate constants (k_a and k_d) were derived by global fit of sensorgrams to 1:1 Langmuir interaction model.

Differential Scanning Fluorimetry (DSF). The thermal melting point (T_m) of the CaMKIIα WT hub was assessed with and without the presence of NCS-382 (5 – 1280 μM), **1b** (1.25 – 320 μM), and Ph-HTBA (0.625 – 160 μM by differential scanning fluorimetry on a Mx3005P qPCR system (Agilent Technologies). CaMKIIα WT hub protein (0.1 mg/ml), compounds and 8x SYPRO® Orange Protein Gel Stain (Life Technologies, #S6650) was diluted in 2-(N-morpholino)ethanesulfonic acid (MES) buffer (20 mM MES, 150 NaCl, 1 mM DTT, pH 6) in 96-well qPCR plates (25 μg/well). Fluorescence was monitored in 85 cycles with a 1 °C temperature increase per minute (25–100 °C) using excitation at 492 nm and emission at 610 nm. T_m values were acquired by fitting the sigmoidal curves of normalized fluorescence intensity to the Boltzmann equation in GraphPad Prism (v. 9). The difference in T_m (ΔT_m) comparing compound concentration to CaMKIIα WT hub was plotted against compound concentration to generate concentration-response curves. Maximum ΔT_m was obtained *via* non-linear regression using 'One site-Fit logIC_{50}'. Data were obtained from at least three independent experiments performed in singlicates.

Intrinsic Tryptophan Fluorescence (ITF; Trp flip) Assay. Human 6x hub recombinant purified protein (final concentration of 5.2 μM) and compounds (NCS-382, Ph-HTBA and **1k**) were diluted in assay buffer (10 mM HEPES pH 7.4, 150 mM NaCl, 1 mM DTT) and mixed in a microplate. For absorbance and background fluorescence measurements, compounds were mixed with buffer for each compound concentration. All measurements were recorded at 25 °C on a Safire plate reader (Tecan) using black 96-well OptiPlates (PerkinElmer) for fluorescence and ½-area UV-Star microplates (#675801, Greiner Bio-One) for absorbance. Emission was recorded in the wavelength range of 300-450 nm with 1 nm increments and an excitation wavelength of 290 nm with 5 nm band widths. Fluorescence intensities at 340 nm

were used for data analysis. Additionally, the absorbance was measured in the range of 270-400 nm to check for inner filter correction. Whereas NCS-382 showed no interference, Ph-HTBA and **1k** displayed a significant interference with fluorescence. The fluorescence for Ph-HTBA and **1k** was corrected for inner filter effect according to:

$$F_{corrected} = (F_{obs} - F_b) * 10^{(0.5*h(A_{290\,nm}+A_{340\,nm}))}$$

where F_{obs} is the observed fluorescence intensity and F_b is the background fluorescence for compound in buffer alone, h is the height of the well adjusted to the sample volume in cm, and A is absorbance at 290 or 340 nm.

Fluorescence intensities and generation of concentration-response curves were normalized according to:

$$F = \frac{(F_{obs} - F_b) - F_{min}}{F_{max} - F_{min}}$$

where F_{obs} represents the observed fluorescence intensity and F_b the background fluorescence for compound in buffer alone. F_{max} corresponds to the maximal fluorescence intensity of hub alone without compound, and F_{min} describes the fluorescence intensity when a bottom plateau is reached at high compound concentrations in the presence of hub. For Ph-HTBA, the corrected fluorescence intensities were used for normalization. Since Ph-HTBA did not reach a plateau at high compound concentrations, F_{min} was set to the fluorescence intensity of buffer for all compounds tested. Fluorescence intensities usually spanned from 5,000-59,000 for Ph-HTBA, while the fluorescence intensity for buffer was around 1000. Data analysis was performed using GraphPad Prism, v. 8. Data were fitted to the equation for '*log(inhibitor) vs. response with variable slope'* to determine IC_{50} values. All data points for Ph-HTBA were performed in five technical replicates using at least two different aliquots of protein as specified in the respective figure legends. Data points for NCS-382 and **1k** were obtained from technical duplicates.

***In Vitro* Metabolic Studies of Ph-HTBA.** *In vitro* metabolic stability studies of Ph-HTBA were performed in mouse and human liver microsomes in a 96-well plate (Porvair, UK) by using the RSP Freedom EVO (Tecan, Swiss) and Hamilton (Hamilton, MA) systems, and in mouse and human hepatocytes in a 48-well plate (Becton Dickinson Labware, USA) using the RSP Freedom EVO systems. The Ph-HTBA sodium salt (at a final concentration of 0.5 μM) was incubated at 37 °C for at least 5 min in liver microsomes at 0.5 mg/mL protein concentration in the presence of NADPH regeneration system, and in hepatocytes at the cell concentration of 0.5 x 10^6 cells/mL. At various time points, Tecan EVO system took 50 μL aliquots of the incubation microsome samples at 0, 3, 10, 15, 30, and 45 min; while 30 μL of the incubation mixture in hepatocytes samples at 0, 5, 10, 15, 20, 30, 45, 60, 90 and 120 min. Each aliquot was transferred into a 96-well plate (Porvair, UK, Cat. No. 219002) containing cold acetonitrile to quench the reaction. After centrifuging for 10 min at 3000 rpm, the supernatants were collected and diluted for the LC-MS/MS analysis. Test and reference compounds were quantified based on the peak area ratio between the analyst and the internal standard. Verapamil (CYP3A4 substrate) and dextromethorphan (CYP2D6 substrate) were used as positive controls in the microsome assays, while testosterone (Phase I metabolism) and 7-OH coumarin (Phase II metabolism) were used as control for the hepatocyte incubation.

Data Analysis. The intrinsic clearance (CLi) values in liver microsomes and hepatocytes were determined according to the following equations:

$$\text{Microsome CLi} = k * V/M$$

where k represents the observed rate constant for parent degradation, V is the incubation volume and M is the the amount of microsomal proteins in the incubation. Values for microsome CLi are expressed as μL/min/mg liver microsomes.

$$\text{Hepatocyte CLi} = -0.693/ T_{½} * \text{mL incubation/million cells} * 1000$$

where $T_{½}$ represents the half-life of the test compound. Values for hepatocyte CLi are expressed as μL/min/million cells.

***In Vitro* MDCK Transport Studies of Ph-HTBA.** Madin-Darby canine kidney clone-II (MDCK-II) cell lines transfected with human P-gp (MDR1) or BCRP transporter (purchased from SOLVO Biotechnology) were seeded in 96-transwell HTS plates. The Ph-HTBA sodium salt (3 μM) was applied to the apical (A) or basolateral (B) compartment. Additionally, the P-gp transporter inhibitor elacridar (10 μM) or the BCRP transporter inhibitor Ko143 (1 μM) was added to MDCKII-MDR1 cells or MDCKII-BCRP cells, respectively. After preincubation (15 to 30 minutes) in the presence or absence of the inhibitor, the permeation of Ph-HTBA in the direction of A→B or B→A was determined in triplicate over a 60- or 90-min incubation at 37 °C and 5% CO_2 with a relative humidity of 95%. At the end of the incubation period, the samples were extracted by protein precipitation with acetonitrile containing rolipram (for the positive ion mode) or diclofenac (for the negative ion mode) as generic internal standard compounds and centrifuged for 10 min at 3000 rpm. The supernatants were collected and diluted for the LC-MS/MS analysis. Test and reference compounds were quantified based on the peak area ratio between the analyst and the internal standard.

Data Analysis. The apparent permeability coefficient (Papp) was determined according to the following equation:

$$Papp(nm/\sec) = \left(\frac{dQ}{dt}\right) x \left(\frac{1}{C0}\right) x \left(\frac{1}{A}\right)$$

where dQ/dt represents the permeability rate, C_0 is the initial concentration in the donor solution (expressed as the ratio for the internal standard ratio) and A is the surface area of the cell monolayer.

The efflux ratios were calculated using the following equation:

$$EffluxRatio = \left(\frac{B - APapp(nm/\sec)}{A - BPapp(nm/\sec)} \right)$$

***In Vivo* Measurements in General.** *In vivo* experiments were performed by Aptuit, Evotec (Verona, Italy). Ethical permission for the *in vivo* studies were subject to legislation under the Italian Legislative Decree no. 26/2014 in accordance with the Directive 2010/63/EU of the European Parliament and of the Council and under authorization issued by the Italian Ministry of Health (internal code no. 38200, modulo B: BH1 and BH2).

***In Vivo* Metabolic Study of Ph-HTBA.** *In vivo* metabolic fate of Ph-HTBA was evaluated in male C57BL/6J mice (25−30 g, Charles River Laboratories). The sodium salt of Ph-HTBA was dissolved in an aqueous solution containing 5% DMSO, 10% Solutol and 85% water, and administered intravenously at a dose of 1 mg/kg. Plasma concentrations of Ph-HTBA were assessed at 0.083, 0.25, 0.5, 1, 2, 4, 8 and 24 h (n = 3) post drug administration. All blood samples were collected into 50 µL of Li Heparine capillary (Minivette POCT) through the mouse tail vein and immediately transferred into polypropylene eppendorf tubes. Blood samples were stored on wet ice until centrifugation for 10 min at 3000 x *g* at 4 °C to obtain plasma samples. Subsequently, 10 µL of the plasma was transferred into micronic tubes and mixed with 40 µL of 0.1N HEPES solution. All plasma samples were stored at -20 °C until bioanalysis. Quantitative bioanalysis was performed using HPLC-MS/MS. Test and reference compounds were quantified based on the peak area ratio between the analyst and the internal standard.

***In Vivo* Brain Exposure Study of Ph-HTBA.** Plasma and brain exposures of Ph-HTBA were evaluated in male C57BL/6J mice (20−25 g, Charles River Laboratories). The sodium salt of Ph-HTBA was dissolved in 2% hydroxypropyl methylcellulose (HPMC), 1% Tween 80 in water, and administered orally at a dose of 10 mg/kg. Brain-to-plasma distributions of Ph-HTBA were assessed at 30 min (n = 3) post drug administration. The animals were anesthetized by isoflurane and blood samples were collected into heparinized tubes through cava vein followed by decapitation. Brains were gently removed and rinsed on filter paper. Blood samples were stored on wet ice until centrifugation for 10 min at 3000 x *g* at 4 °C to obtain plasma samples. Plasma and brain samples were stored at -20 °C until bioanalysis. Brain homogenate was prepared by homogenizing the whole brain using isothermal focused acoustic ultrasonication (Covaris Inc., Woburn, MA) in water (1:4 v/v). Quantitative bioanalysis was performed using HPLC-MS/MS. Test and reference compounds were quantified based on the peak area ratio between the analyst and the internal standard.

Computational Modeling. *Ligand and Protein Preparation*. The 2D chemical structures of the compounds were built in Maestro Schrödinger and default settings in LigPrep (**Schrödinger Release 2021-2**: LigPrep, Schrödinger, LLC, New York, NY, 2021) were used to generate accurate, energy minimized 3D molecular structures. Protonation states, tautomeric forms and partial charges of the ligands were assigned using Epik[52,53] in the OPLS3[54] forcefield. The in-house obtained (PDB: 7REC) co-crystal structure of CaMKIIα/5-HDC[5] was prepared using the Protein Preparation Wizard[55] including a hydrogen optimization at pH = 7.4 of the ionizable polar groups using Maestro PROPKA.[55]

Molecular Docking. Glide[56-58] was used (SP and XP) with default settings to dock all ligands. Rotation of hydroxyl hydrogen atoms in the binding site was allowed, and the options to enhance the planarity of conjugated π-systems, and to include the Epik state penalties to the scoring calculations were further selected. Flexible ligand sampling was applied combined with

the biased sampling of amide groups (penalization of nonplanar conformations). The docking grid centroid was placed around the co-crystallized ligand 5-HDC in the binding cavity of the hub domain, and the cubic grid box sides were set at 10 Å. All 3D images were produced in PyMOL (The PyMOL Molecular Graphics System, Version 2.0 Schrödinger, LLC).

ASSOCIATED CONTENT

Supporting information. The Supporting Information is available free of charge.

Molecular formula strings (CSV)

Concentration-response curves of [^{3}H]NCS-382 displacement (Figure S1), surface plasmon resonance binding of NCS-382, **1b** and Ph-HTBA (**1i**) (Figure S2), thermal shift assessment of NCS-382 and **1b** (Figure S3), intrinsic tryptophan fluorescence measurement of **1k** (Figure S4), *in vivo* metabolic evaluation of Ph-HTBA after intravenous administration to mice (Figure S5), analytical HPLC traces of **1b**, **1k**, Ph-HTBA and the sodium salt of Ph-HTBA (Figure S6), and summarized SPR kinetic parameters for NCS-382, **1b**, and Ph-HTBA (Table S1).

AUTHOR INFORMATION

Corresponding Authors

* Chemistry: Prof. Bente Frølund - Phone: +45 35336495; email: bfr@sund.ku.dk

* Pharmacology & biophysics: Prof. Petrine Wellendorph - Phone: +45 35336397; email: pw@sund.ku.dk

ORCIDs

Bente Frølund: https://orcid.org/0000-0001-5476-6288

Mohamed A. Shehata: https://orcid.org/0000-0001-5475-1967

Petrine Wellendorph: https://orcid.org/0000-0002-5455-8013

Sara Solbak: https://orcid.org/0000-0003-0233-7160

Yongsong Tian: https://orcid.org/0000-0001-7084-9083

Author Contributions

B.F. and P.W. did conceptualization and obtained project funding. Y.T. and M.A.S. are as main project contributors considered joined co-first authors of this paper. Y.T., C.V. and J.S.R. synthesized all compounds, and M.A.S. designed analogs and performed computational chemistry modelling. S.J.G., L.H., S.S. and P.W. designed and developed the pharmacology and biophysics assays. S.J.G., L.H., L.T., J.B.-J., U.L., A.S.G.L., S.S. and P.W. performed bioassays and data analysis. The manuscript was written by Y.T, M.A.S., S.J.G., P.W. and B.F. with contributions from all authors. All authors have given approval to the final version of the manuscript.

Notes

The authors declare the following competing financial interest. Y.T, M.A.S. S.J.G., L.H., L.T., J.B.-J., J.S.R., A.S.G.L., J.K., and S.S. have no conflicts of interest to disclose. B.F., P.W. and U.L: International Patent WO/2019/149329.

ACKNOWLEDGMENT

The authors would like to thank Prof. John Kuriyan for plasmids for CaMKIIα hub protein expression and helpful comments on the project. This work was supported through financial support from the following foundations and grants: The Lundbeck Foundation (grants R277-2018-260 to P.W., R303-2018-3162 to M.A.S), The Novo Nordisk Foundation (grants ECO

and NNF19SA0057841), the Independent Research Fund Denmark (1026-00335B to P.W.), and the Drug Research Academy for a Lundbeck Foundation pre-graduate scholarship in pharmaceutical neuroscience to A.S.G.L.

ABBREVIATIONS

5-HDC, 5-hydroxydiclofenac; BBB, blood-brain barrier; BCRP, breast cancer resistance protein; CaMKIIα, Ca^{2+}/calmodulin-dependent protein kinase II alpha; DSF, differential scanning fluorimetry; GHB, γ-hydroxybutyric acid; HOCPCA, 3-hydroxycyclopenten-1-enecarboxylic acid; ITF, intrinsic tryptophan fluorescence; MCT-1, monocarboxylate transporter 1; NCS-382, (*E*)-2-(5-hydroxy-5,7,8,9-tetrahydro-6*H*-benzo[7]-annulen-6-ylidene)acetic acid; P-gp, P-glycoprotein; Ph-HTBA, (*E*)-2-(5-hydroxy-2-phenyl-5,7,8,9-tetrahydro-6*H*-benzo[7]annulen-6-ylidene)acetic acid; SAR, structure-affinity relationship; SEM, standard error of the mean; SPR, surface plasmon resonance; TSA, thermal shift assay; UDP, uridine diphosphate; UGT2B7, UDP glucuronosyltransferase family 2 member B7.

REFERENCES

(1) Bernasconi, R.; Mathivet, P.; Bischoff, S.; Marescaux, C., Gamma-hydroxybutyric acid: an endogenous neuromodulator with abuse potential? *Trends in Pharmacol. Sci.* **1999,** *20*, 135-141.

(2) Xu, X.-M.; Wei, Y.-D.; Liu, Y.; Li, Z.-X., Gamma-hydroxybutyrate (GHB) for narcolepsy in adults: an updated systematic review and meta-analysis. *Sleep Medicine* **2019,** *64*, 62-70.

(3) Mannucci, C.; Pichini, S.; Spagnolo, V. E.; Calapai, F.; Gangemi, S.; Navarra, M.; Calapai, G., Sodium oxybate therapy for alcohol withdrawal syndrome and keeping of alcohol abstinence. *Current Drug Metabolism* **2018,** *19*, 1056-1064.

(4) Robinson, D. M.; Keating, G. M., Sodium oxybate: a review of its use in the management of narcolepsy. *CNS Drugs* **2007,** *21*, 337-354.

(5) Leurs, U.; Klein, A. B.; McSpadden, E. D.; Griem-Krey, N.; Solbak, S. M. Ø.; Houlton, J.; Villumsen, I. S.; Vogensen, S. B.; Hamborg, L.; Gauger, S. J.; Palmelund, L. B.; Larsen, A. S. G.; Shehata, M. A.; Kelstrup, C. D.; Olsen, J. V.; Bach, A.; Burnie, R. O.; Kerr, D. S.; Gowing, E. K.; Teurlings, S. M. W.; Chi, C. C.; Gee, C. L.; Frølund, B.; Kornum, B. R.; van Woerden, G. M.; Clausen, R. P.; Kuriyan, J.; Clarkson, A. N.; Wellendorph, P., GHB analogs confer neuroprotection through specific interaction with the CaMKIIα hub domain. *Proceedings of the National Academy of Sciences* **2021,** *118*, e2108079118.

(6) Tian, Y.; Shehata, M. A.; Gauger, S. J.; Ng, C. K. L.; Solbak, S.; Thiesen, L.; Bruus-Jensen, J.; Krall, J.; Bundgaard, C.; Gibson, K. M.; Wellendorph, P.; Frølund, B., Discovery and optimization of 5-hydroxydiclofenac toward a new class of ligands with nanomolar affinity for the CaMKIIα hub domain. *J. Med. Chem.* **2022,** *65*, 6656–6676.

(7) Rosenberg, O. S.; Deindl, S.; Sung, R.-J.; Nairn, A. C.; Kuriyan, J., Structure of the autoinhibited kinase domain of CaMKII and SAXS analysis of the holoenzyme. *Cell* **2005,** *123*, 849-860.

(8) Brocke, L.; Chiang, L. W.; Wagner, P. D.; Schulman, H., Functional implications of the subunit composition of neuronal CaM kinase II. *J. Biol. Chem.* **1999,** *274*, 22713-22722.

(9) Cook, S. G.; Bourke, A. M.; O'Leary, H.; Zaegel, V.; Lasda, E.; Mize-Berge, J.; Quillinan, N.; Tucker, C. L.; Coultrap, S. J.; Herson, P. S.; Bayer, K. U., Analysis of the CaMKIIα and β splice-variant distribution among brain regions reveals isoform-specific differences in holoenzyme formation. *Scientific Reports* **2018,** *8*, 5448.

(10) Erondu, N.; Kennedy, M., Regional distribution of type II Ca2+/calmodulin-dependent protein kinase in rat brain. *The Journal of Neuroscience* **1985,** *5*, 3270-3277.

(11) Hell, Johannes W., CaMKII: claiming center stage in postsynaptic function and organization. *Neuron* **2014,** *81*, 249-265.

(12) Coultrap, Steven J.; Freund, Ronald K.; O'Leary, H.; Sanderson, Jennifer L.; Roche, Katherine W.; Dell'Acqua, Mark L.; Bayer, K. U., Autonomous CaMKII mediates both LTP and LTD using a mechanism for differential substrate site selection. *Cell Reports* **2014,** *6*, 431-437.

(13) Lisman, J.; Yasuda, R.; Raghavachari, S., Mechanisms of CaMKII action in long-term potentiation. *Nature Reviews Neurosci.* **2012,** *13*, 169-182.

(14) Coultrap, S. J.; Bayer, K. U., CaMKII regulation in information processing and storage. *Trends in Neurosci.* **2012,** *35*, 607-618.

(15) Hansel, C.; de Jeu, M.; Belmeguenai, A.; Houtman, S. H.; Buitendijk, Gabriëlle H. S.; Andreev, D.; De Zeeuw, Chris I.; Elgersma, Y., αCaMKII is essential for cerebellar LTD and motor learning. *Neuron* **2006,** *51*, 835-843.

(16) Coultrap, S. J.; Vest, R. S.; Ashpole, N. M.; Hudmon, A.; Bayer, K. U., CaMKII in cerebral ischemia. *Acta Pharmacologica Sinica* **2011,** *32*, 861-872.

(17) Rostas, J. A. P.; Spratt, N. J.; Dickson, P. W.; Skelding, K. A., The role of Ca2+-calmodulin stimulated protein kinase II in ischaemic stroke – a potential target for neuroprotective therapies. *Neurochem. Intern.* **2017,** *107*, 33-42.

(18) Ghosh, A.; Giese, K. P., Calcium/calmodulin-dependent kinase II and Alzheimer's disease. *Mol Brain* **2015,** *8*, 78-78.

(19) Moriguchi, S.; Yabuki, Y.; Fukunaga, K., Reduced calcium/calmodulin-dependent protein kinase II activity in the hippocampus is associated with impaired cognitive function in MPTP-treated mice. *J. Neurochem.* **2012,** *120*, 541-551.

(20) Küry, S.; van Woerden, G. M.; Besnard, T.; Proietti Onori, M.; Latypova, X.; Towne, M. C.; Cho, M. T.; Prescott, T. E.; Ploeg, M. A.; Sanders, S.; Stessman, H. A. F.; Pujol, A.; Distel, B.; Robak, L. A.; Bernstein, J. A.; Denommé-Pichon, A.-S.; Lesca, G.; Sellars, E. A.; Berg, J.; Carré, W.; Busk, Ø. L.; van Bon, B. W. M.; Waugh, J. L.; Deardorff, M.; Hoganson, G. E.; Bosanko, K. B.; Johnson, D. S.; Dabir, T.; Holla, Ø. L.; Sarkar, A.; Tveten, K.; de Bellescize, J.; Braathen, G. J.; Terhal, P. A.; Grange, D. K.; van Haeringen, A.; Lam, C.; Mirzaa, G.; Burton, J.; Bhoj, E. J.; Douglas, J.; Santani, A. B.; Nesbitt, A. I.; Helbig, K. L.; Andrews, M. V.; Begtrup, A.; Tang, S.; van Gassen, K. L. I.; Juusola, J.; Foss, K.; Enns, G. M.; Moog, U.; Hinderhofer, K.; Paramasivam, N.; Lincoln, S.; Kusako, B. H.; Lindenbaum, P.; Charpentier, E.; Nowak, C. B.; Cherot, E.; Simonet, T.; Ruivenkamp, C. A. L.; Hahn, S.; Brownstein, C. A.; Xia, F.; Schmitt, S.; Deb, W.; Bonneau, D.; Nizon, M.; Quinquis, D.; Chelly, J.; Rudolf, G.; Sanlaville, D.; Parent, P.; Gilbert-Dussardier, B.; Toutain, A.; Sutton, V. R.; Thies, J.; Peart-Vissers, L. E. L. M.; Boisseau, P.; Vincent, M.; Grabrucker, A. M.; Dubourg, C.; Tan, W.-H.; Verbeek, N. E.; Granzow, M.; Santen, G. W. E.; Shendure, J.; Isidor, B.; Pasquier, L.; Redon, R.; Yang, Y.; State, M. W.; Kleefstra, T.; Cogné, B.; Petrovski, S.; Retterer, K.; Eichler, E. E.; Rosenfeld, J. A.; Agrawal, P. B.; Bézieau, S.; Odent, S.; Elgersma, Y.; Mercier, S., De novo mutations in protein kinase genes CAMK2A and CAMK2B cause intellectual disability. *The American Journal of Human Genetics* **2017,** *101*, 768-788.

(21) Pellicena, P.; Schulman, H., CaMKII inhibitors: from research tools to therapeutic agents. *Frontiers in Pharmacology* **2014,** *5*.

(22) Neef, S.; Mann, C.; Zwenger, A.; Dybkova, N.; Maier, L. S., Reduction of SR Ca2+ leak and arrhythmogenic cellular correlates by SMP-114, a novel CaMKII inhibitor with oral bioavailability. *Basic Research in Cardiology* **2017,** *112*, 45.

(23) Neef, S.; Steffens, A.; Pellicena, P.; Mustroph, J.; Lebek, S.; Ort, K. R.; Schulman, H.; Maier, L. S., Improvement of cardiomyocyte function by a novel pyrimidine-based CaMKII-inhibitor. *Journal of Molecular and Cellular Cardiology* **2018,** *115*, 73-81.

(24) Vest, R. S.; Davies, K. D.; O'Leary, H.; Port, J. D.; Bayer, K. U., Dual mechanism of a natural CaMKII inhibitor. *Molecular Biology of the Cell* **2007,** *18*, 5024-5033.

(25) Wong, M. H.; Samal, A. B.; Lee, M.; Vlach, J.; Novikov, N.; Niedziela-Majka, A.; Feng, J. Y.; Koltun, D. O.; Brendza, K. M.; Kwon, H. J.; Schultz, B. E.; Sakowicz, R.; Saad, J. S.; Papalia, G. A., The KN-93 molecule inhibits calcium/calmodulin-dependent protein kinase II (CaMKII) activity by binding to Ca2+/CaM. *J. Mol. Biol.* **2019,** *431*, 1440-1459.

(26) Sloutsky, R.; Dziedzic, N.; Dunn, M. J.; Bates, R. M.; Torres-Ocampo, A. P.; Boopathy, S.; Page, B.; Weeks, J. G.; Chao, L. H.; Stratton, M. M., Heterogeneity in human hippocampal CaMKII transcripts reveals allosteric hub-dependent regulation. *Sci Signal* **2020,** *13*, 1-12.

(27) Stratton, M.; Lee, I.-H.; Bhattacharyya, M.; Christensen, S. M.; Chao, L. H.; Schulman, H.; Groves, J. T.; Kuriyan, J., Activation-triggered subunit exchange between CaMKII holoenzymes facilitates the spread of kinase activity. *eLife* **2014,** *3*, e01610.

(28) Bhattacharyya, M.; Stratton, M. M.; Going, C. C.; McSpadden, E. D.; Huang, Y.; Susa, A. C.; Elleman, A.; Cao, Y. M.; Pappireddi, N.; Burkhardt, P.; Gee, C. L.; Barros, T.; Schulman, H.; Williams, E. R.; Kuriyan, J., Molecular mechanism of activation-triggered subunit exchange in Ca2+/calmodulin-dependent protein kinase II. *eLife* **2016,** *5*, e13405.

(29) McSpadden, E. D.; Xia, Z.; Chi, C. C.; Susa, A. C.; Shah, N. H.; Gee, C. L.; Williams, E. R.; Kuriyan, J., Variation in assembly stoichiometry in non-metazoan homologs of the hub domain of Ca2+/calmodulin-dependent protein kinase II. *Protein Science* **2019,** *28*, 1071-1082.

(30) Hoelz, A.; Nairn, A. C.; Kuriyan, J., Crystal structure of a tetradecameric assembly of the association domain of Ca2+/calmodulin-dependent kinase II. *Molecular Cell* **2003,** *11*, 1241-1251.

(31) Wellendorph, P.; Høg, S.; Greenwood, J. R.; de Lichtenberg, A.; Nielsen, B.; Frølund, B.; Brehm, L.; Clausen, R. P.; Bräuner-Osborne, H., Novel cyclic gamma-hydroxybutyrate (GHB) analogs with high affinity and stereoselectivity of binding to GHB sites in rat brain. *J. Pharmacol. Exp. Ther.* **2005,** *315*, 346-351.

(32) Krall, J.; Bavo, F.; Falk-Petersen, C. B.; Jensen, C. H.; Nielsen, J. O.; Tian, Y.; Anglani, V.; Kongstad, K. T.; Piilgaard, L.; Nielsen, B.; Gloriam, D. E.; Kehler, J.; Jensen, A. A.; Harpsøe, K.; Wellendorph, P.; Frølund, B., Discovery of 2-(imidazo[1,2-b]pyridazin-2-yl)acetic acid as a new class of ligands selective for the γ-hydroxybutyric acid (GHB) high-affinity binding sites. *J. Med. Chem.* **2019,** *62*, 2798-2813.

(33) Høg, S.; Wellendorph, P.; Nielsen, B.; Frydenvang, K.; Dahl, I. F.; Bräuner-Osborne, H.; Brehm, L.; Frølund, B.; Clausen, R. P., Novel high-affinity and selective biaromatic 4-substituted γ-hydroxybutyric acid (GHB) analogues as GHB ligands: design, synthesis, and binding studies. *J. Med. Chem.* **2008,** *51*, 8088-8095.

(34) Krall, J.; Jensen, C. H.; Bavo, F.; Falk-Petersen, C. B.; Haugaard, A. S.; Vogensen, S. B.; Tian, Y.; Nittegaard-Nielsen, M.; Sigurdardóttir, S. B.; Kehler, J.; Kongstad, K. T.; Gloriam, D. E.; Clausen, R. P.; Harpsøe, K.; Wellendorph, P.; Frølund, B., Molecular hybridization of potent and selective γ-hydroxybutyric acid (GHB) ligands: design, synthesis, binding Studies, and molecular modeling of novel 3-hydroxycyclopent-1-enecarboxylic acid (HOCPCA) and trans-γ-hydroxycrotonic acid (T-HCA) analogs. *J. Med. Chem.* **2017,** *60*, 9022-9039.

(35) Vogensen, S. B.; Marek, A.; Bay, T.; Wellendorph, P.; Kehler, J.; Bundgaard, C.; Frølund, B.; Pedersen, M. H. F.; Clausen, R. P., New synthesis and tritium labeling of a

selective ligand for studying high-affinity γ-hydroxybutyrate (GHB) binding sites. *J. Med. Chem.* **2013,** *56*, 8201-8205.

(36) Thiesen, L.; Kehler, J.; Clausen, R. P.; Frølund, B.; Bundgaard, C.; Wellendorph, P., In vitro and in vivo evidence for active brain uptake of the GHB analog HOCPCA by the monocarboxylate transporter subtype 1. *J. Pharmacol. Exp. Ther.* **2015,** *354*, 166-174.

(37) Thiesen, L.; Belew, Z. M.; Griem-Krey, N.; Pedersen, S. F.; Crocoll, C.; Nour-Eldin, H. H.; Wellendorph, P., The γ-hydroxybutyric acid (GHB) analogue NCS-382 is a substrate for both monocarboxylate transporters subtypes 1 and 4. *Eur. J. Pharm. Sci.* **2020,** *143*, 105203.

(38) Maitre, M.; Hechler, V.; Vayer, P.; Gobaille, S.; Cash, C. D.; Schmitt, M.; Bourguignon, J. J., A specific gamma-hydroxybutyrate receptor ligand possesses both antagonistic and anticonvulsant properties. *J. Pharmacol. Exp. Ther.* **1990,** *255*, 657-663.

(39) Bay, T.; Eghorn, L. F.; Klein, A. B.; Wellendorph, P., GHB receptor targets in the CNS: focus on high-affinity binding sites. *Biochem. Pharmacol.* **2014,** *87*, 220-228.

(40) Castelli, M. P.; Mocci, I.; Pistis, M.; Peis, M.; Berta, D.; Gelain, A.; Gessa, G. L.; Cignarella, G., Stereoselectivity of NCS-382 binding to γ-hydroxybutyrate receptor in the rat brain. *Eur. J. Pharmacol.* **2002,** *446*, 1-5.

(41) Murineddu, G.; Ruiu, S.; Loriga, G.; Manca, I.; Lazzari, P.; Reali, R.; Pani, L.; Toma, L.; Pinna, G. A., Tricyclic pyrazoles. 3. synthesis, biological evaluation, and molecular modeling of analogues of the cannabinoid antagonist 8-chloro-1-(2‘,4‘-dichlorophenyl)-N-piperidin-1-yl-1,4,5,6-tetrahydrobenzo[6,7]cyclohepta[1,2-c]pyrazole-3-carboxamide. *J. Med.Chem.* **2005,** *48*, 7351-7362.

(42) Tang, P.; Furuya, T.; Ritter, T., Silver-catalyzed late-stage fluorination. *J. Am. Chem. Soc.* **2010,** *132*, 12150-12154.

(43) Blevins, D. W.; Yao, M.-L.; Yong, L.; Kabalka, G. W., Iododemetallation of potassium organotrifluoroborates and tributylarylstannanes using sodium iodide/iron(III) chloride. *Tet. Let.* **2015,** *56*, 3130-3132.

(44) Ono, M.; Haratake, M.; Mori, H.; Nakayama, M., Novel chalcones as probes for in vivo imaging of β-amyloid plaques in Alzheimer's brains. *Bioorg. Med. Chem.* **2007,** *15*, 6802-6809.

(45) Bayer, K. U.; De Koninck, P.; Leonard, A. S.; Hell, J. W.; Schulman, H., Interaction with the NMDA receptor locks CaMKII in an active conformation. *Nature* **2001,** *411*, 801-805.

(46) Strack, S.; McNeill, R. B.; Colbran, R. J., Mechanism and regulation of calcium/calmodulin-dependent protein kinase II targeting to the NR2B subunit of the N-methyl-d-aspartate receptor. *J. Biol.Chem.* **2000,** *275*, 23798-23806.

(47) Hudmon, A.; LeBel, E.; Roy, H.; Sik, A.; Schulman, H.; Waxham, M. N.; De Koninck, P., A mechanism for Ca2+/calmodulin-dependent protein kinase II clustering at synaptic and nonsynaptic sites based on self-association. *The Journal of Neuroscience* **2005,** *25*, 6971-6983.

(48) Lin, F.-Y.; MacKerell, A. D., Do halogen–hydrogen bond donor interactions dominate the favorable contribution of halogens to ligand–protein binding? *The Journal of Physical Chemistry B* **2017,** *121*, 6813-6821.

(49) Cavallo, G.; Metrangolo, P.; Milani, R.; Pilati, T.; Priimagi, A.; Resnati, G.; Terraneo, G., The halogen bond. *Chemical Reviews* **2016,** *116*, 2478-2601.

(50) Ainslie, G. R.; Gibson, K. M.; Vogel, K. R., A pharmacokinetic evaluation and metabolite identification of the GHB receptor antagonist NCS-382 in mouse informs novel therapeutic strategies for the treatment of GHB intoxication. *Pharmacol. Res. Perspect.* **2016,** *4*, 1-10.

(51) Sagar, A.; Anika, M. S. H.; William, F. E.; Bjorn, B., Breast cancer resistance protein and P-glycoprotein in brain cancer: two gatekeepers team up. *Current Pharmaceutical Design* **2011,** *17*, 2793-2802.

(52) Greenwood, J. R.; Calkins, D.; Sullivan, A. P.; Shelley, J. C., Towards the comprehensive, rapid, and accurate prediction of the favorable tautomeric states of drug-like molecules in aqueous solution. *Journal of Computer-Aided Molecular Design* **2010,** *24*, 591-604.

(53) Shelley, J. C.; Cholleti, A.; Frye, L. L.; Greenwood, J. R.; Timlin, M. R.; Uchimaya, M., Epik: a software program for pKaprediction and protonation state generation for drug-like molecules. *Journal of Computer-Aided Molecular Design* **2007,** *21*, 681-691.

(54) Harder, E.; Damm, W.; Maple, J.; Wu, C.; Reboul, M.; Xiang, J. Y.; Wang, L.; Lupyan, D.; Dahlgren, M. K.; Knight, J. L.; Kaus, J. W.; Cerutti, D. S.; Krilov, G.; Jorgensen, W. L.; Abel, R.; Friesner, R. A., OPLS3: a force field providing broad coverage of drug-like small molecules and proteins. *Journal of Chemical Theory and Computation* **2016,** *12*, 281-296.

(55) Madhavi Sastry, G.; Adzhigirey, M.; Day, T.; Annabhimoju, R.; Sherman, W., Protein and ligand preparation: parameters, protocols, and influence on virtual screening enrichments. *Journal of Computer-Aided Molecular Design* **2013,** *27*, 221-234.

(56) Friesner, R. A.; Murphy, R. B.; Repasky, M. P.; Frye, L. L.; Greenwood, J. R.; Halgren, T. A.; Sanschagrin, P. C.; Mainz, D. T., Extra precision glide: docking and scoring incorporating a model of hydrophobic enclosure for protein−ligand complexes. *J. Med. Chem.* **2006,** *49*, 6177-6196.

(57) Friesner, R. A.; Banks, J. L.; Murphy, R. B.; Halgren, T. A.; Klicic, J. J.; Mainz, D. T.; Repasky, M. P.; Knoll, E. H.; Shelley, M.; Perry, J. K.; Shaw, D. E.; Francis, P.; Shenkin,

P. S., Glide: a new approach for rapid, accurate docking and scoring. 1. Method and assessment of docking accuracy. *J. Med. Chem.* **2004,** *47*, 1739-1749.

(58) Halgren, T. A.; Murphy, R. B.; Friesner, R. A.; Beard, H. S.; Frye, L. L.; Pollard, W. T.; Banks, J. L., Glide: a new approach for rapid, accurate docking and scoring. 2. Enrichment factors in database screening. *J. Med.Chem.* **2004,** *47*, 1750-1759.